RESERVOIR SIMULATION AND EVALUATION OF THE UPPER JURASSIC SMACKOVER MICROBIAL CARBONATE AND GRAINSTONE-PACKSTONE RESERVOIRS IN LITTLE CEDAR CREEK FIELD, CONECUH COUNTY, ALABAMA

A Thesis

by

MOETAZ YOUSSEF GHONAMEE MOSTAFA

Submitted to the Office of Graduate Studies of
Texas A&M University
in partial fulfillment of the requirements for the degree of

MASTER OF SCIENCE

Approved by:

Chair of Committee, Ernest A.Mancini
Co-Chair of Committee, Duane A. McVay
Committee Members, Michael C.Pope
Yuefeng Sun
Head of Department, John R. Giardino

May 2013

Major Subject: Geology

ABSTRACT

This thesis presents an integrated study of mature carbonate oil reservoirs (Upper Jurassic Smackover Formation) undergoing gas injection in the Little Cedar Creek Field located in Conecuh County, Alabama. This field produces from two reservoirs, one grainstone-packstone and the other microbial boundstone. The main objective of the study is to determine a potential redevelopment plan to increase oil recovery from the field by targeting the remaining oil saturation. This study involves using numerical reservoir simulation to identify the remaining recoverable oil distribution throughout the field. The 3-D geological model, which served as input for the dynamic reservoir simulation performed in this study, was provided by another author.

Reservoir simulation indicates that potentially high recoverable oil saturation remains in the unitized area in the southwestern part of the field. Also, the simulation studies show that the following redevelopment plan investigated in this study has the potential to recover up to 5 MMSTB of oil by January 2017: converting 3 wells to inject water into the microbial boundstone reservoir, converting one more well to inject recycled gas into the grainstone-packstone reservoir performing work-over operations on 18 wells, sidetracking a plugged and abandoned well 10560, already completed in the grainstone-packstone reservoir, to another location in the same reservoir, and drilling 7 new wells in the grainstone-packstone reservoir and 5 new wells in the microbial boundstone reservoir. All these 12 new wells should be drilled on 160-acre unit size according to the field rules. Moreover, reservoir simulation showed that drilling additional 6 wells on a unit size less than160-acre (infill drilling) could result in additional recovery of up to 0.7 MMSTB of oil from the grainstone-packstone reservoir. No cost-benefit analysis studies have been performed in this thesis. Thus, the redevelopment plan investigated cannot be recommended for implementation until such analyses have been conducted.

DEDICATION

I dedicated this thesis to my father (Mr. Youssef Mostafa), my mother (Enshrah El Lithy), my brother (Mohammed Mostafa), my brother (Moaaz Mostafa) and my sister (May Mostafa) for their endless love and support.

ACKNOWLEDGEMENTS

The author would like to thank Dr. Ernest A. Mancini for his endless support during my study at Texas A&M University and for supervising my master thesis. He was such a great adviser and mentor, and I am proud to be his last graduate student. Also, I would like to thank Dr. Duane A. McVay for serving as co-chair of the thesis; he was the first one who introduced me to the uncertainty assessment that is used in petroleum industry. Special thanks to both Dr. Michael Pope and Dr. Yuefeng Sun for being committee members.

Great appreciation should go to both ExxonMobil Company for sponsoring my study through the award of a Middle East and North Africa (MENA) scholarship, and personnel of the International Institute of Education (IIE) (especially David DeGroot) for managing the scholarship. Finally, I would like to thank my family and friends, especially Hassan Salama and Mostafa Siam, for their support and motivation.

TABLE OF CONTENTS

LIST OF FIGURES

FIGURE Page

FIGURE Page

LIST OF TABLES

INTRODUCTION

The Little Cedar Creek Field is in Conecuh County, Alabama (**Figs. 1** and **2**). In this field, the Upper Jurassic Smackover Formation overlies conglomerate and sandstone facies of the Norphlet Formation and underlies the argillaceous, anhydritic carbonaceous facies of the Haynesville Formation. The structure map on the top of Smackover Formation in the Little Cedar Creek Field shows that the Smackover Formation dips from the northeast to southwest, and structural closure is not evident. The petroleum trap in the Little Cedar Creek Field is a stratigraphic trap near the updip depositional limit of Smackover Formation as a result of facies changes both laterally and vertically (Mancini et al., 2008).

Seven lithofacies occur in the Smackover Formation in the Little Cedar Creek Field Ridgway (2010). From top to bottom, these lithofacies are: 1) peritidal lime mudstone; 2) tidal channel floatstone-rudstone; 3) peloid-ooid shoal grainstone-packstone; 4) subtidal wackestone; 5) microbially-influenced packstone; 6) microbial (thrombolite) boundstone; and 7) transgressive lime mudstone-dolostone. The shoal grainstone-packstone and the microbial boundstone are the two proven reservoir facies in the Little Cedar Creek Field. The peritidal lime mudstone and the transgressive lime mudstone-dolostone are vertical and lateral seals for the two reservoirs. The subtidal wackestone serves as a vertical seal, separating the two reservoirs and inhibiting pressure communication.

The Little Cedar Creek Field was discovered in 1994 by Hunt Oil Company when well 10560 was drilled and completed in the grainstone-packstone reservoir (Mancini et al., 2008). This well produced up to 108 BPD of 46°API oil (Mancini et al., 2008). The field remained as a single-well field until 2000 when substantial drilling was started by Midroc Operating Company and Sklar Operating Company. Currently, Pruet Production and Sklar Operating Company operate in the field. The first oil production from the microbial boundstone reservoir was in 2004

when well permit 13438 was drilled and completed. The field produced under primary depletion until 2007. The southwestern portion of the Little Cedar Creek Field was unitized in January of

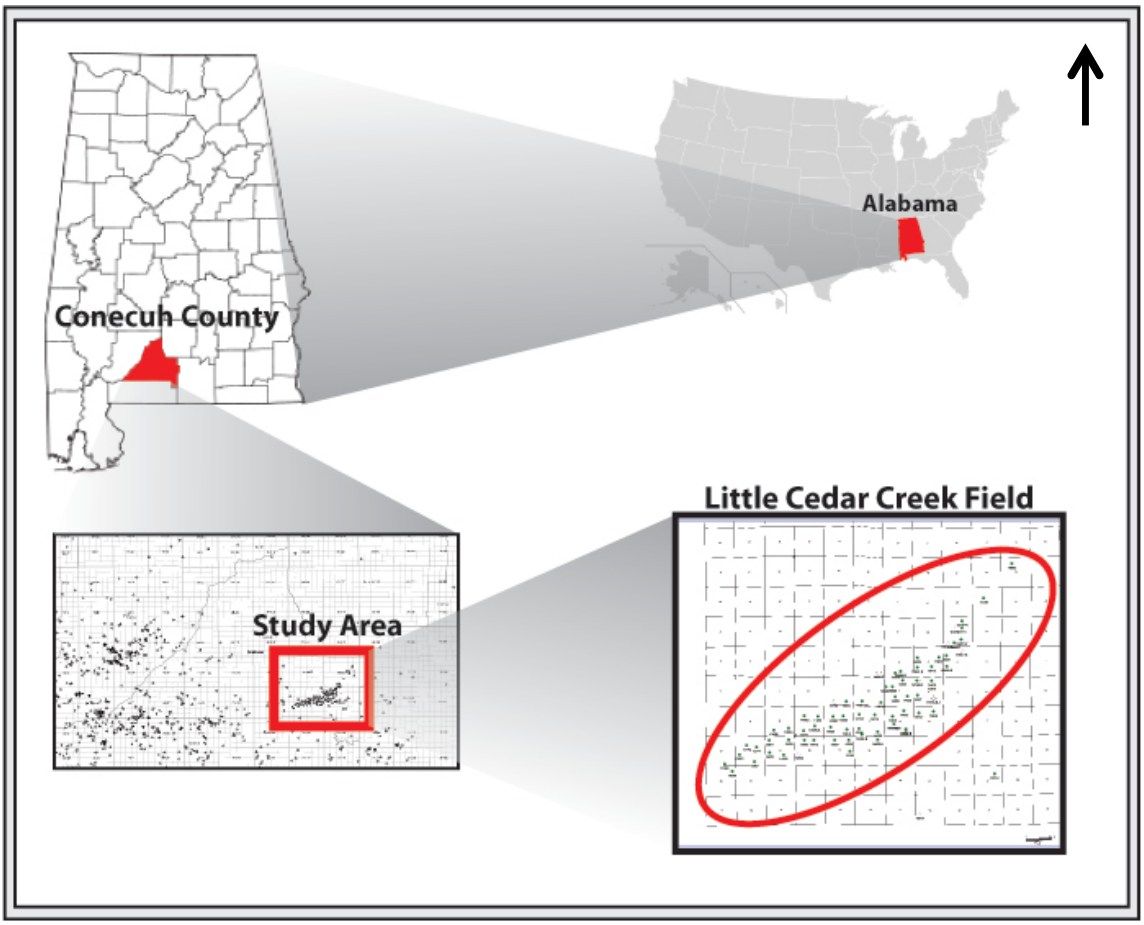

Fig. 1 — Location of Little Cedar Creek Field , Conecuh County, Alabama (Ridgway, 2010).

of 2005 (a map of the field and unit area can be viewed at http://www.ogb.state.al.us/apps/ogb_maps/). In August 2007, two wells were converted into gas injectors in the unitized area to keep the grainstone-packstone reservoir pressure from declining further (State Oil and Gas Board of Alabama, November 2010). At the time of study, a third well was converted into an injection well. Through February 2012, about 100 wells were drilled in the Little Cedar Creek Field, resulting in cumulative oil production of 13.2 MMBBL and 13.7 MMSCF of natural gas. Some wells produce from only one reservoir, while other wells produce from both

reservoirs. The volumetric estimated OOIP is 90 MMSTB. The purpose of this study is to integrate the reservoir characterization provided by Ridgeway (2010) and the 3-D geologic model provided by AL Haddad (2012) with the 3-D reservoir simulation model performed in this study to determine a potential redevelopment plan.

GEOLOGIC SETTING

The Smackover Formation in the Little Cedar Creek Field was deposited on the western edge of the Conecuh embayment (subbasin) as part of the Oxfordian marine transgression-regression (Ridgway, 2010). The tectonic setting of the Mississippi interior salt basin and the Manila and the Conecuh embayments are related to the evolution of the Gulf of Mexico (Wood and Walper, 1974). The Conecuh and the Manila embayments and the Mississippi interior salt basin are the major negative features, associated with the evolution of the Gulf of Mexico, in southwest Alabama (Mancini et al., 1995).

The evolution of Gulf of Mexico is characterized by extensional rift tectonics and involved two phases: rifting and drifting. The drifting phase of the Gulf of Mexico included the formation of new oceanic crust followed by the rotational migration of Yucatan to its present position relative to North America during the Callovian–Valanginian (Pindell, 2010). During this drifting phase, the extensional and the isostatic adjustment of the oceanic crust, due to the separation of the North American plate from the South American and African plates, produced the overall configuration of the Gulf (MacRae et al., 1993). As a result of this tectonic activity, a broad zone of attenuated thick transitional crust formed along the northeastern margin of the Gulf of Mexico. Within this zone of attenuated crust, a pattern of alternating basement highs and lows, which represents areas of greater or lesser attenuation, occurred. The Mississippi Interior salt basin and the Manila and Conecuh subbasins formed over basement lows. Structural highs, such as the Sabine uplift, the Monroe uplift, the Wiggins arch, the LaSalle arch, the Choctaw ridge complex, and the Conecuh ridge complex, act to separate the basins and subbasins (Mancini, et al. 2008; **Fig. 2**). The evolution of the Conecuh Ridge complex is attributed to the late Paleozoic convergence of the North American and African-South American continental plates associated with the Appalachian fold-and thrust structural trend (Mancini et al., 2003).

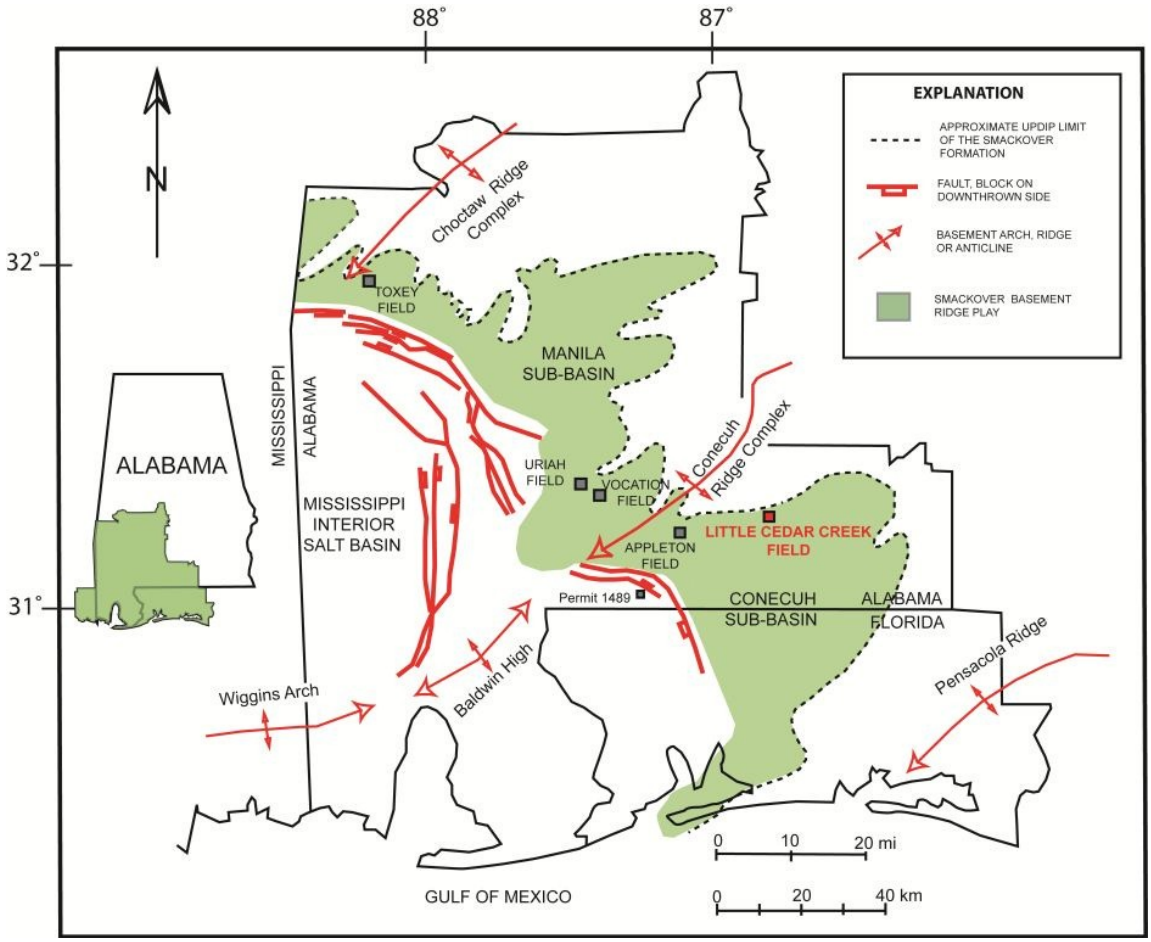

Fig. 2 — Major structural features and key Smackover fields (Mancini et al., 2008).

The depositional events in the northeastern Gulf of Mexico, including in the Manila and the Conecuh embayments, were related to the rifting and opening of the Gulf of Mexico (Mancini et al., 2001). During the Late Jurassic (Oxfordian) and following the widespread deposition of salt, major marine transgression occurred due to the emplacement of the new oceanic crust, sea-floor spreading and subsequent thermal subsidence of the Gulf of Mexico due to crust cooling (Mancini et al., 2001). The sea-floor spreading and the associated marine transgression terminated salt deposition by creating an open marine environment versus the previous restricted marine condition where salt was deposited (MacRae et al., 1993).

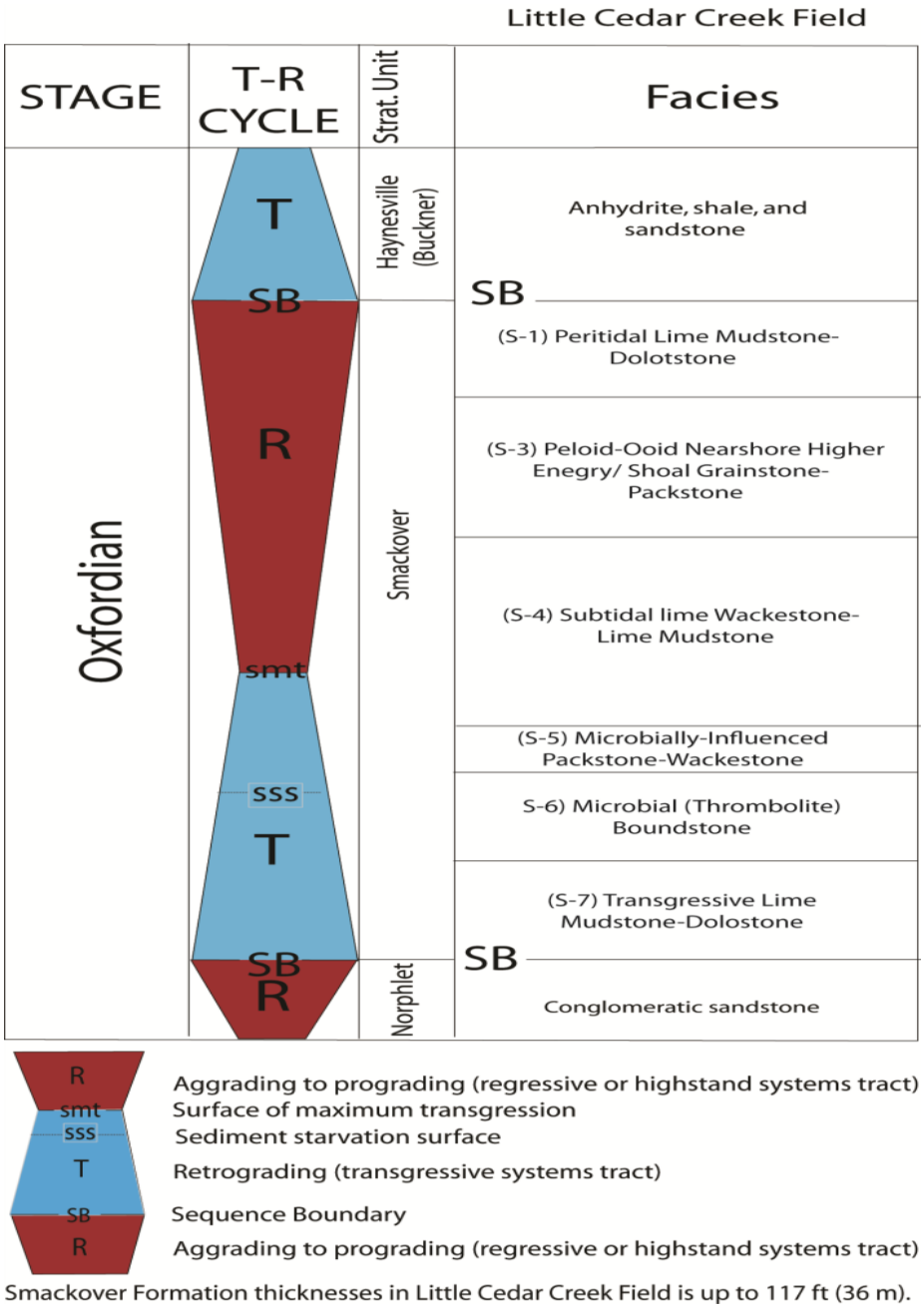

Fig. 3 — Upper Jurassic stratigraphy of the Little Cedar Creek Field (modified from Mancini et al., 2008).

Smackover facies were deposited in the Conecuh embayment and, in turn, in the Little Cedar Creek Field during the Jurassic marine transgression. The deposition of the Smackover Formation followed the deposition of Norphlet Formation sandstones and conglomerates

(MacRae et al., 1993). Locally at Little Cedar Creek Field, the Smackover disconformably overlies the Norphlet Formation (Ridgway, 2010). The Wiggins arch, Baldwin high, and Conecuh and Pensacola ridges served to restrict Smackover deposition in the Conecuh embayment area (Mancini and Benson, 1980). The Haynesville Formation, which overlies the Smackover Formation, consists of carbonates and clastics (**Fig. 3**).

The Smackover Formation was deposited on a carbonate ramp across the northern rim of the Gulf of Mexico (Mancini et al., 2001). In southwestern Alabama, the pre-Smackover structure follows the ramp profile, but paleohighs associated with this ramp affected the lateral facies distribution (Markland, 1992). Major structures influencing and restricting Smackover deposition in the southwestern Alabama area were the Wiggins arch, Choctaw ridge, Conecuh ridge, and Pensacola ridge (Mancini and Benson, 1980; Markland, 1992) The structure map on the top of Smackover Formation at the Little Cedar Creek Field (**Fig. 4**) shows that Smackover beds dip northeast to southwest with no evidence of any structural closure in the field. The petroleum trap is a stratigraphic trap as a result of facies changes both laterally and vertically.

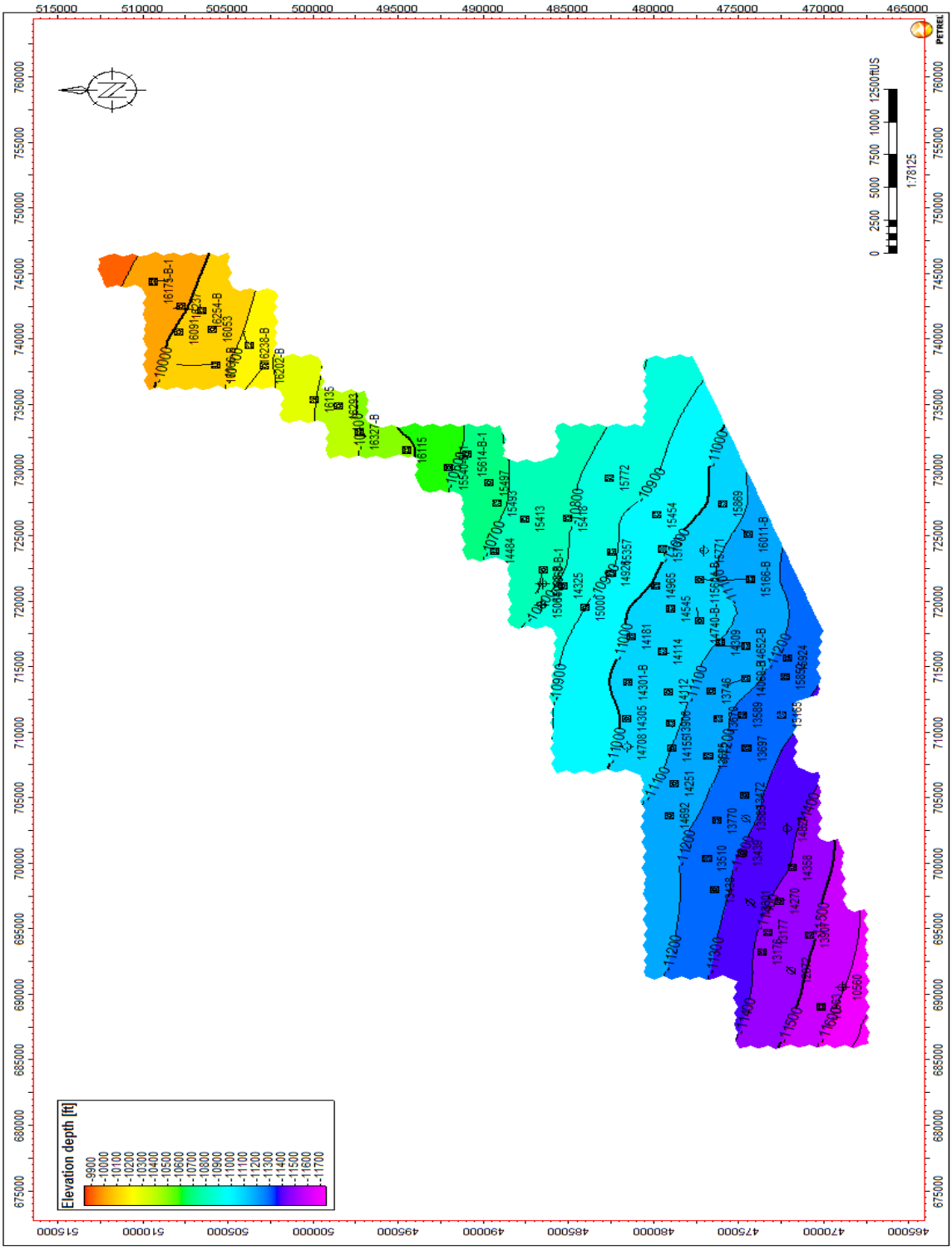

Fig. 4 — Structure map in top of the Smackover Formation at the Little Cedar Creek Field (Contour interval 100ft.)

RESERVOIR CHARACTERIZATION

Mancini et al. (2006) and Ridgway (2010) described the lithofacies in details. The peritidal facies (S-1) consists of grey to light grey mudstone to wackestone lime and dolostone (Ridgeway, 2010). The facies thickness is 0-25 ft, and it exists in the whole field. The depositional environment is interpreted to be an intertidal to subtidal, low-energy, lagoon (Mancini et al., 2006; Ridgeway, 2010). This facies serves as a vertical and lateral seal for the nearshore high energy grainstone-packstone reservoir **(Figs. 5-12)**. The tidal channel facies (S-2) is a grey rudstone to grainstone (Ridgway, 2010). The facies thickness is 10-22 ft, with limited occurrence only in section 5, T5N, R13E (Ridgway, 2010). This facies has been interpreted as a high energy tidal channel environment (Mancini et al., 2006; Ridgeway, 2010).

The nearshore high energy shoal facies (S-3) is interpreted to be a peloid-ooid shoal grainstone-packstone partially dolomitized limestone facies deposited in high-energy, subtidal shoal environment (Mancini et al., 2006; Ridgeway, 2010). The nearshore high energy shoal facies distribution is southwest-to northeast with a thickness of 0-35 ft. Maximum development is in central part of the field area (Mancini et al., 2008). The facies is absent along the southern and northeastern margin of the field (Al Haddad, 2012; **Figs. 5-12**).

The subtidal wackestone-lime mudstone facies (S-4) is a grey to dark grey limestone (Ridgeway, 2010). The facies was deposited in a “relatively deeper-water” (<10 feet), subtidal marine environment (Ridgeway, 2010). The facies is distributed around the whole field with a thickness of 0-112 ft. This facies is the vertical and lateral seals, which encase the microbial boundstone reservoir (Mancini et al., 2008**; Figs. 5-12).** The microbially-influenced packstone-wackestone facies (S-5) is a grey to dark grey limestone. These beds were deposited in subtidal conditions in a marine environment (Ridgeway, 2010). The facies occurs over the entire field area with thickness of 0-34 ft. The wackestone to lime mudstone facies of this unit serve as an updip lateral seal in the northeastern area of the field (Ridgeway, 2010). The microbial

boundstone facies (S-6) is grey to light-grey and tan limestone. This facies was deposited in a low-energy subtidal (<10 feet) setting in an inner carbonate ramp environment (Ridgway, 2010). The facies exists in the entire field with a thickness of 0-40 ft. This facies occurs as localized major microbial buildups that trend southwest to northeast. The stratigraphic cross-sections along depositional strike (**Figs. 10** and **12**) and dip (**Fig. 8**) show that there are three major microbial buildups trending southwest to northeast in the Little Cedar Creek Field area. The microbial facies are thin between each buildup possibly result in an area of restricted fluid communication between the buildup facies reservoir beds.

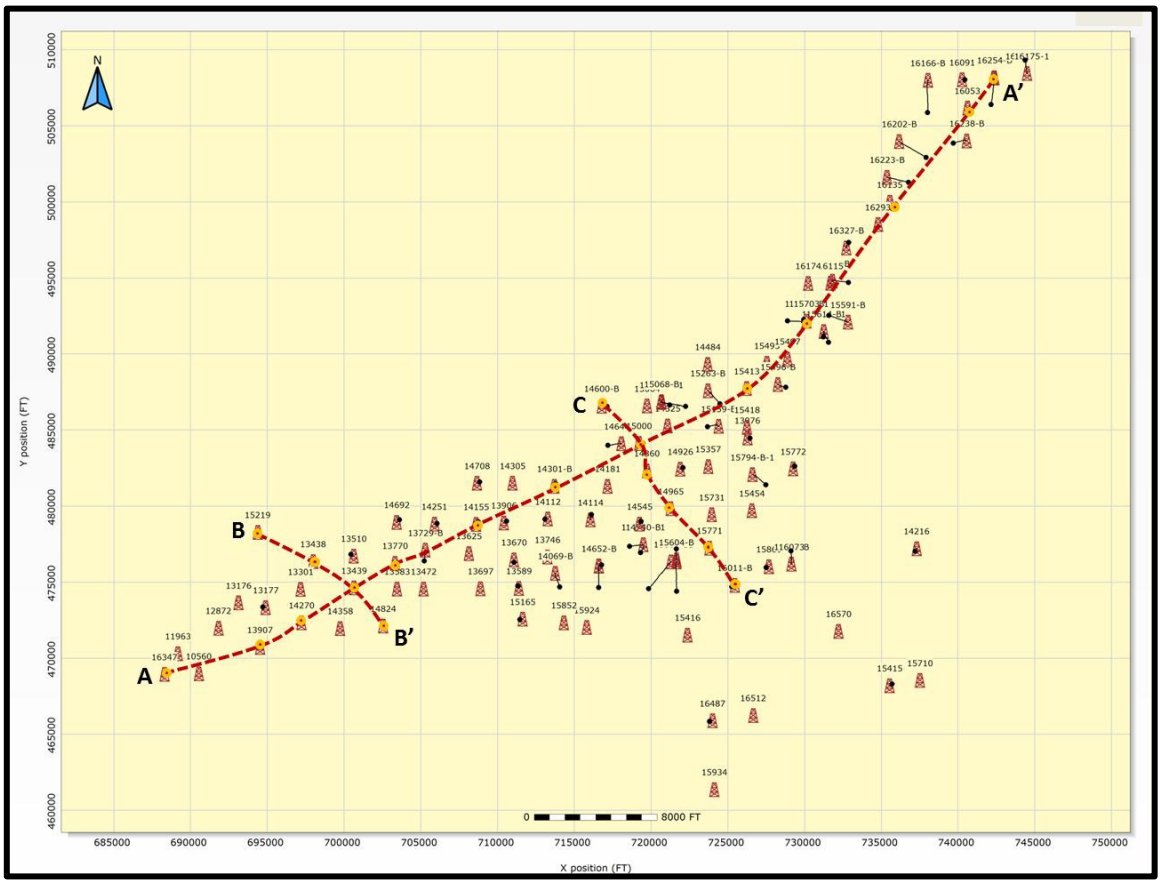

Fig. 5 — Base map of the Little Cedar Creek Field in Alabama (from Al Haddad, 2012).

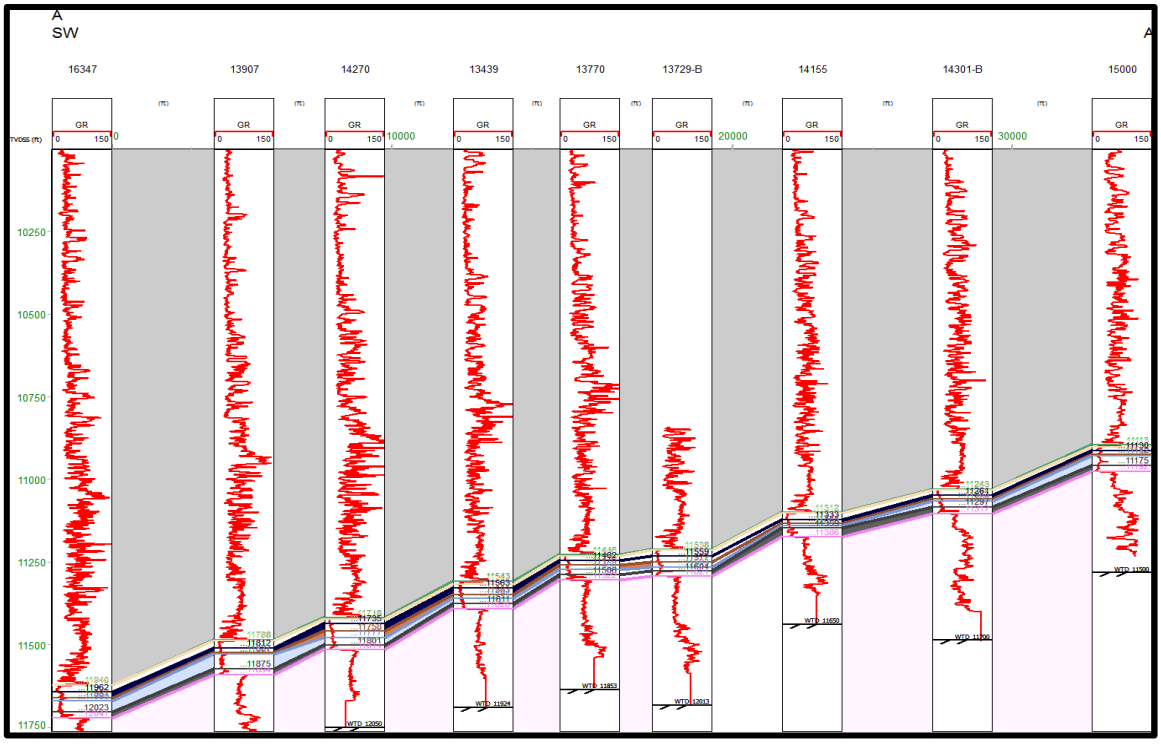

Fig. 6 — A southwest- northeast structural cross section AA' of the Little Cedar Creek Field (Al Haddad, 2012).

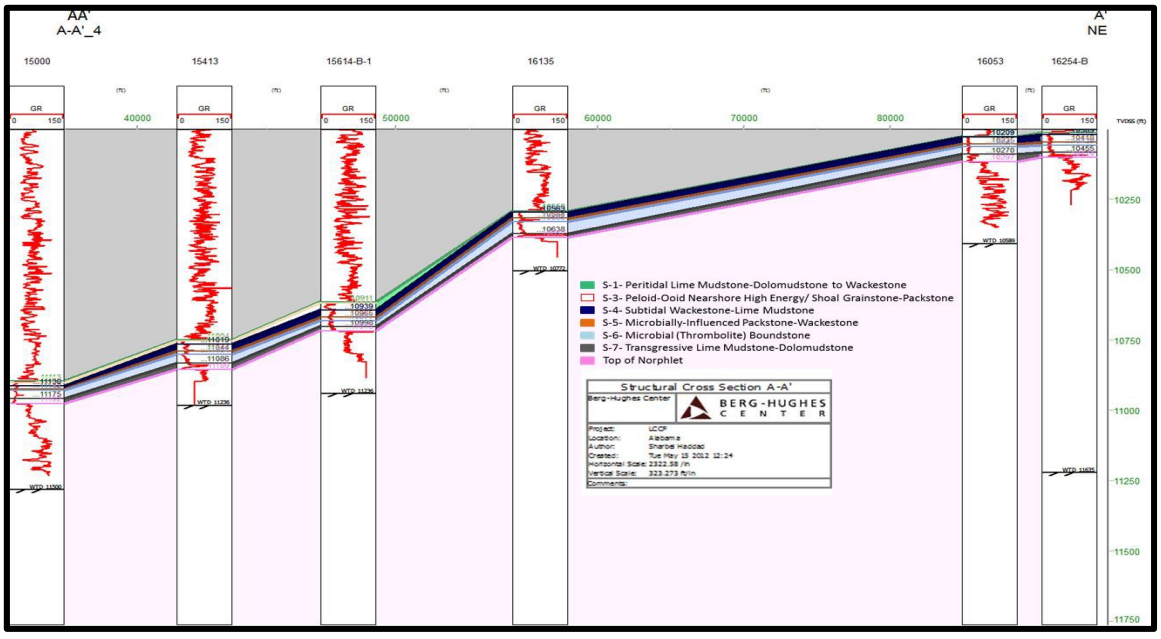

Fig. 7 — Continued southwest- northeast structural cross section (Al Haddad, 2012).

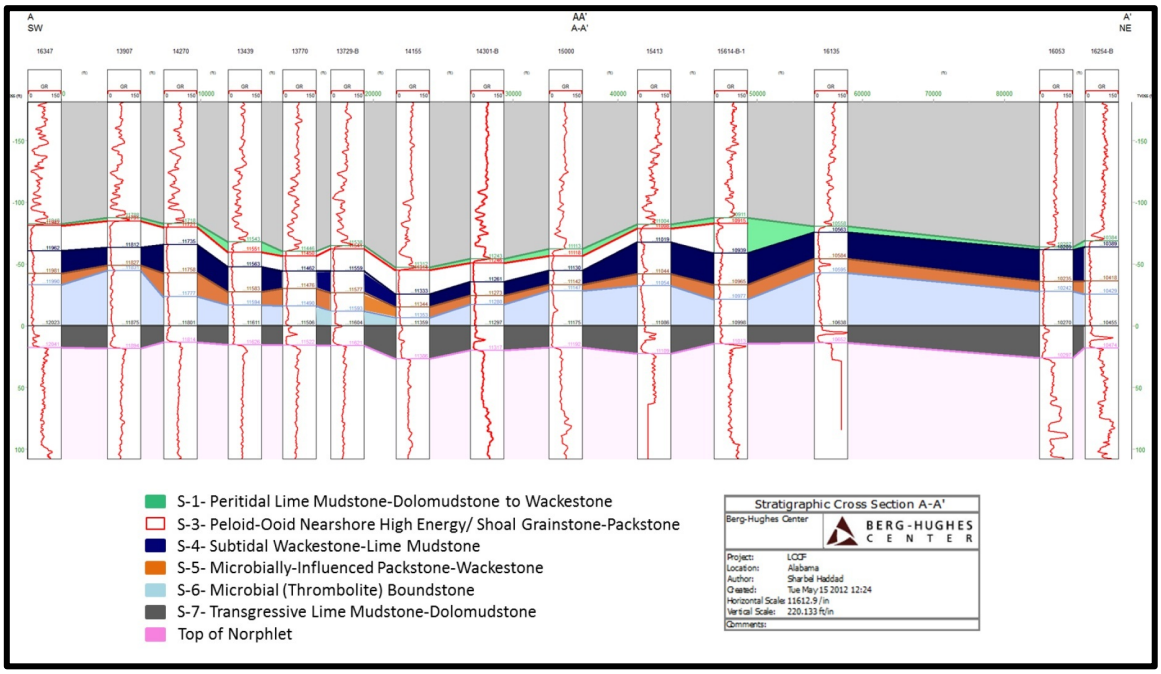

Fig. 8 — Stratigraphic cross section AA' showing the facies in the Little Cedar Creek Field area (Al Haddad, 2012).

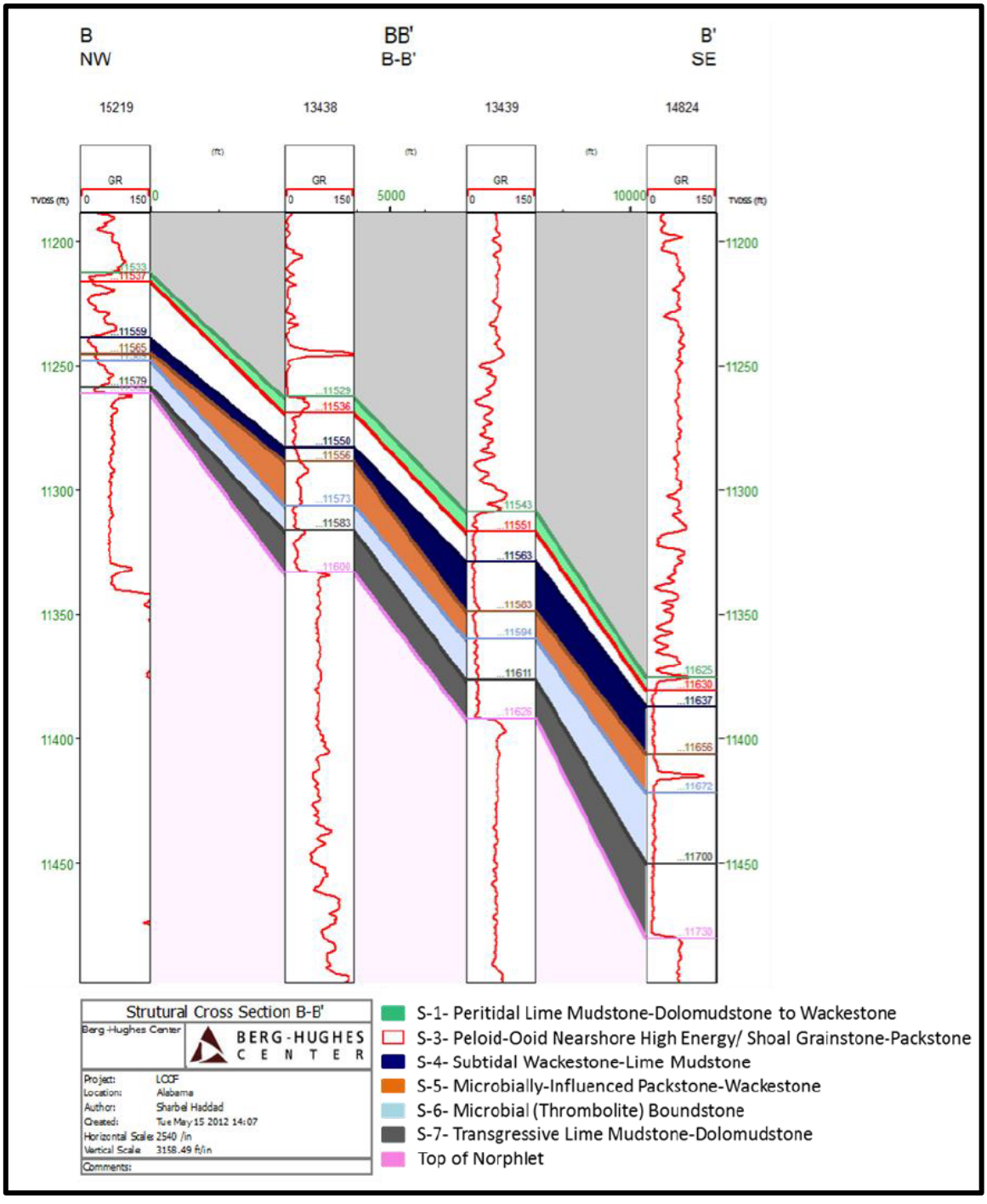

Fig. 9 — A northwest- southeast structural cross section BB' of the Little Cedar Creek Field (Al Haddad, 2012).

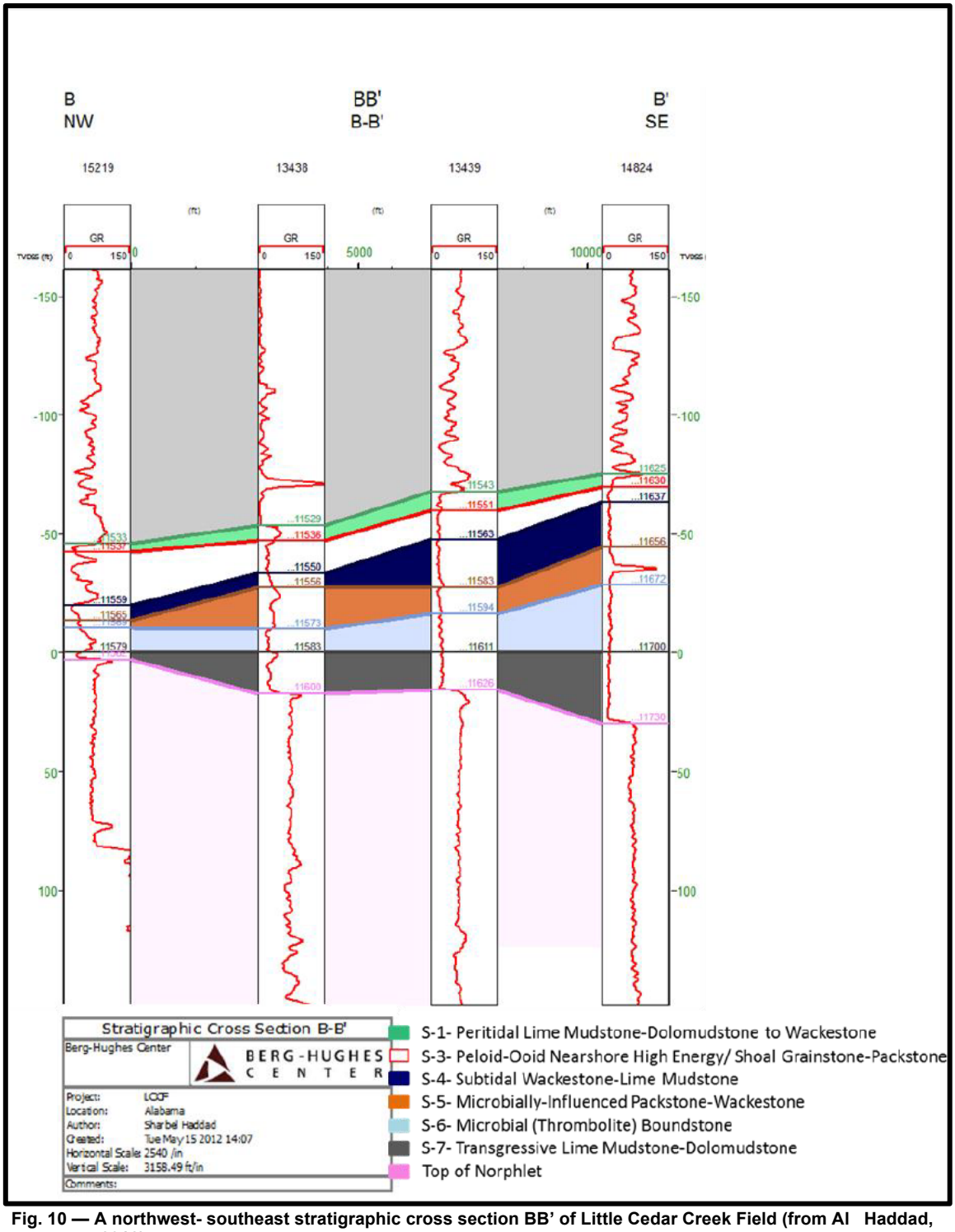

Fig. 10 — A northwest- southeast stratigraphic cross section BB' of Little Cedar Creek Field (from Al Haddad, 2012).

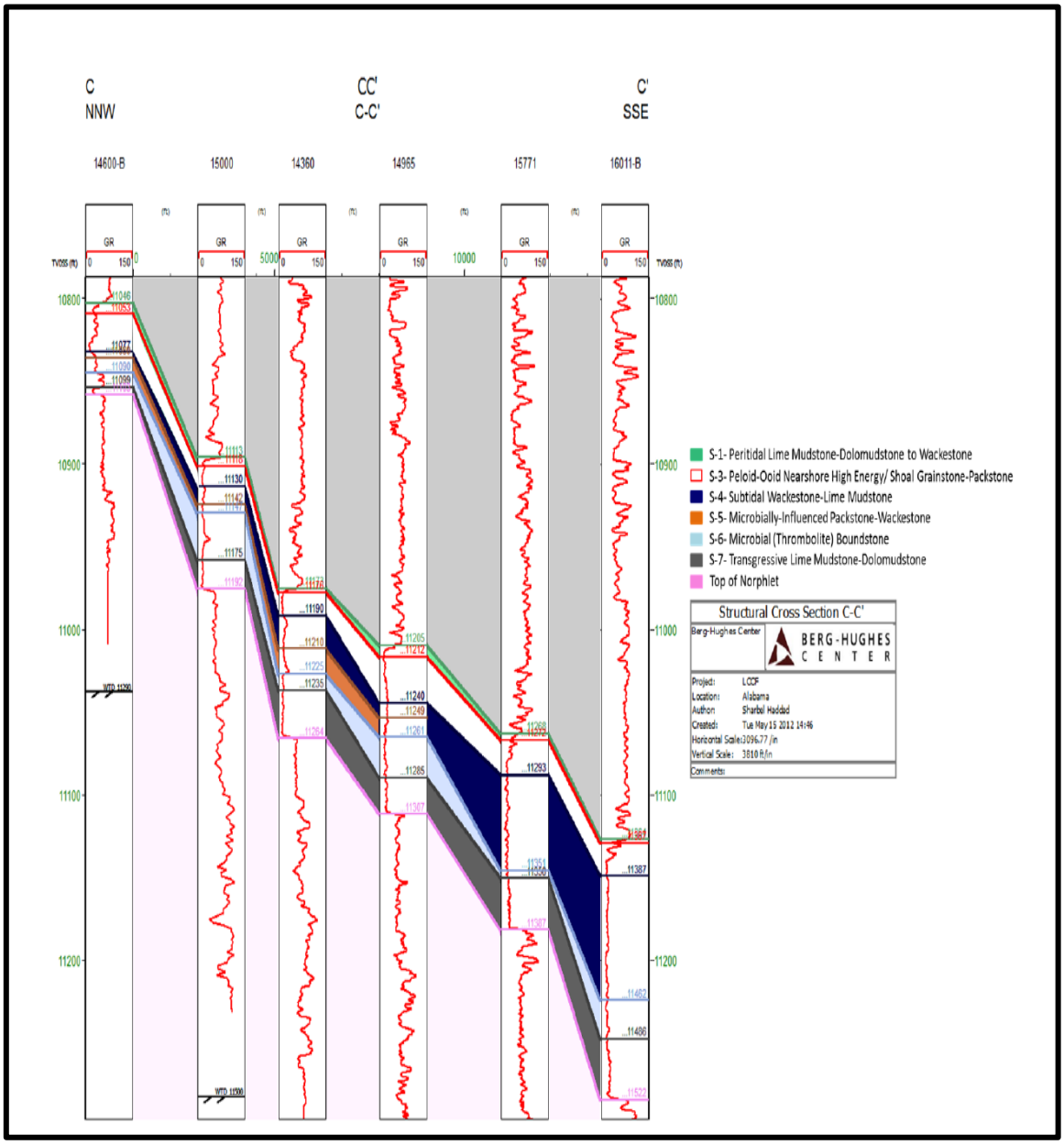

Fig. 11 — A northwest- southeast structural cross section CC' of Little Cedar Creek Field (from Al Haddad, 2012).

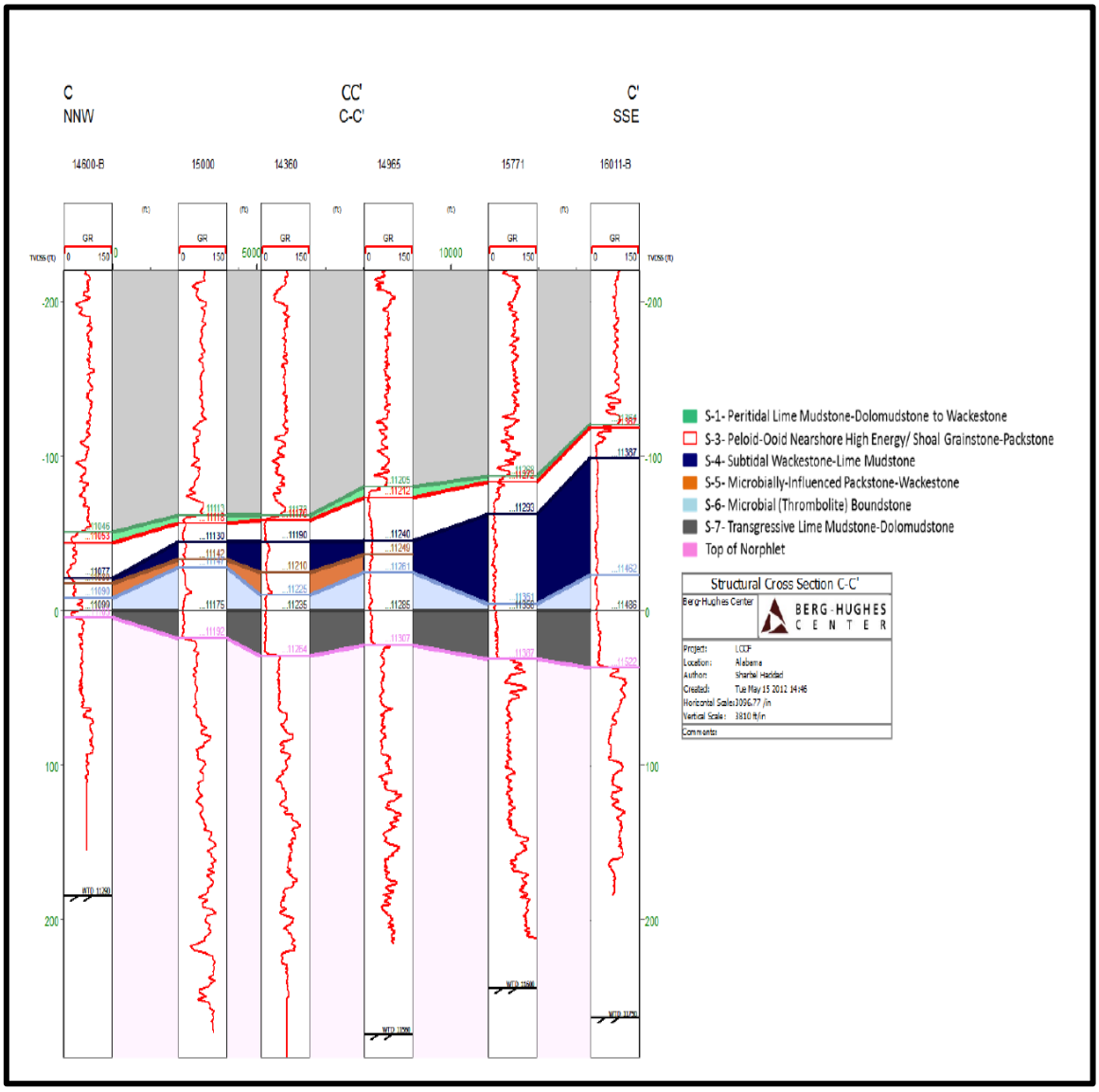

Fig. 12 — A north northwest- south southeast stratigraphic cross section CC' of Little Cedar Creek Field (from Al Haddad, 2012).

The transgressive lime mudstone and dolomudstone facies (S-7) is grey to reddish pink limestone, and the facies occurs over the entire field area, with a thickness of 5-55 ft (Ridgway, 2010). This facies was deposited in the Oxfordian during a relatively rapid marine transgression (Ridgway, 2010).

Depositional fabric is the primary control on reservoir architecture in Smackover carbonates, but diagenesis is a significant factor in modifying reservoir quality (Benson, 1985). Dolomitization and dissolution probably had a significant influence on enhancing the reservoir quality in the Smackover Formation (Mancini et al., 2004). Dolomitization greatly enhances permeability, but this process created only minor amounts of intercrystalline porosity (Benson et al, 1985). The dissolution process enlarges the primary (interparticle) and early secondary (moldic and intercrystalline) pores (McKee, 1990). The dissolution process does not create new pores but expands the existing pore size and thus enhances the permeability (Benson, 1985). The porosity in the grainstone-packstone reservoir in the Little Cedar Creek Field is both primary and secondary (Ridgway, 2010). The porosity is interpreted to be enhanced through partial dolomitization and leaching (Ridgway, 2010). The porosity ranges between 0 and 35%, and the pore type is bimodal (interparticle and intraparticle-to-moldic) (Ridgway, 2010). The permeability range is 0.6-70 md, which is relatively low in comparison to porosity values. The nearshore high-energy shoal grainstone to packstone facies includes up to six cycles of 2-6 ft of wackestone grading upward to packstone-grainstone (Mancini et al., 2008). A total of 21 wells are producing from the grainstone-packstone reservoir with a cumulative oil production ranging from 0.077 to 0.345 MMSTB per well.

The pore types in the microbial boundstone facies are mainly vuggy. The porosity range is (0-30%) and it is associated with high permeability (0-3000 md). The diagenetic (vuggy) porosity greatly enhanced the microbial boundstone reservoir quality in the Little Cedar Creek Field. A total of 33 wells were perforated only in the microbial boundstone reservoir with a cumulative oil production ranging from 0.667 to 47 MMSTB per well.

In the Little Cedar Creek Field, the leached and dolomitized grainstone-packstone reservoir, with interparticle and moldic porosity, has lower reservoir quality than the microbial boundstone reservoir, which is dominated by vuggy and enlarged porosity. The moldic pore system is characterized by a high percentage of small-sized pores, which are poorly interconnected or connected through narrow pore throats, whereas the vuggy pore system is

characterized by highly interconnected large-sized pores with larger and uniform pore throats (Mancini et al., 2004). The range of cumulative oil production per well confirms that the microbial boundstone reservoir is more productive than the grainstone-packstone reservoir in the Little Cedar Creek Field.

3-D GEOLOGICAL MODEL

The 3-D geologic model of Al Haddad (2012) provided the geologic framework for the reservoir simulation. The structural, petrophysical, lithological and stratigraphic models were combined to generate the 3-D geologic model. This model served as the foundation for the 3-D, 3-phase numerical reservoir simulation model.

The tops of the Smackover facies was defined by the type log of the Smackover Formation in the Little Cedar Creek Field (**Fig. 13)** was used to define. Truncated Gaussian Simulation was used to generate the 3-D facies distribution in the Little Cedar Creek field (Al Haddad, 2012). Since facies control porosity and diagenesis is facies selective in the Little Cedar Creek field as published by Ridgway (2010); therefore, porosity in the field was distributed within the facies framework in the geologic model (Al Haddad, 2012). The 3-D porosity model was generated using Sequential Gaussian Simulation (SGS) (Al Haddad, 2012). Core porosity and log-derived porosity at well locations served as data for the SGS. At well locations where no core data were available, permeability was calculated from log-derived porosity using a neural network approach, and SGS with collocated cokriging were used to predict the permeability in inter-wells areas (Al Haddad, 2012).

Uncertainty in 3-D Geologic Model

Structural Model Uncertainty

For the purpose of reservoir simulation, the Little Cedar Creek Field structural model was considered to be less uncertain compared to the petrophysical model. The well spacing in the Little Cedar Creek field is 160 contiguous acres upon which no other producible well is located (Special Field Rules for The Little Cedar Creek field, Conecuh County, Alabama, Amendment

September 29, 2011). With a hundred wells penetrating both reservoirs in the Little Cedar Creek Field, the field structural model has less degree of uncertainty; however, there are still some uncertainties, which result from inaccurate picking of the Smackover tops at the well locations. The structural model uncertainties mainly affect the field OOIP.

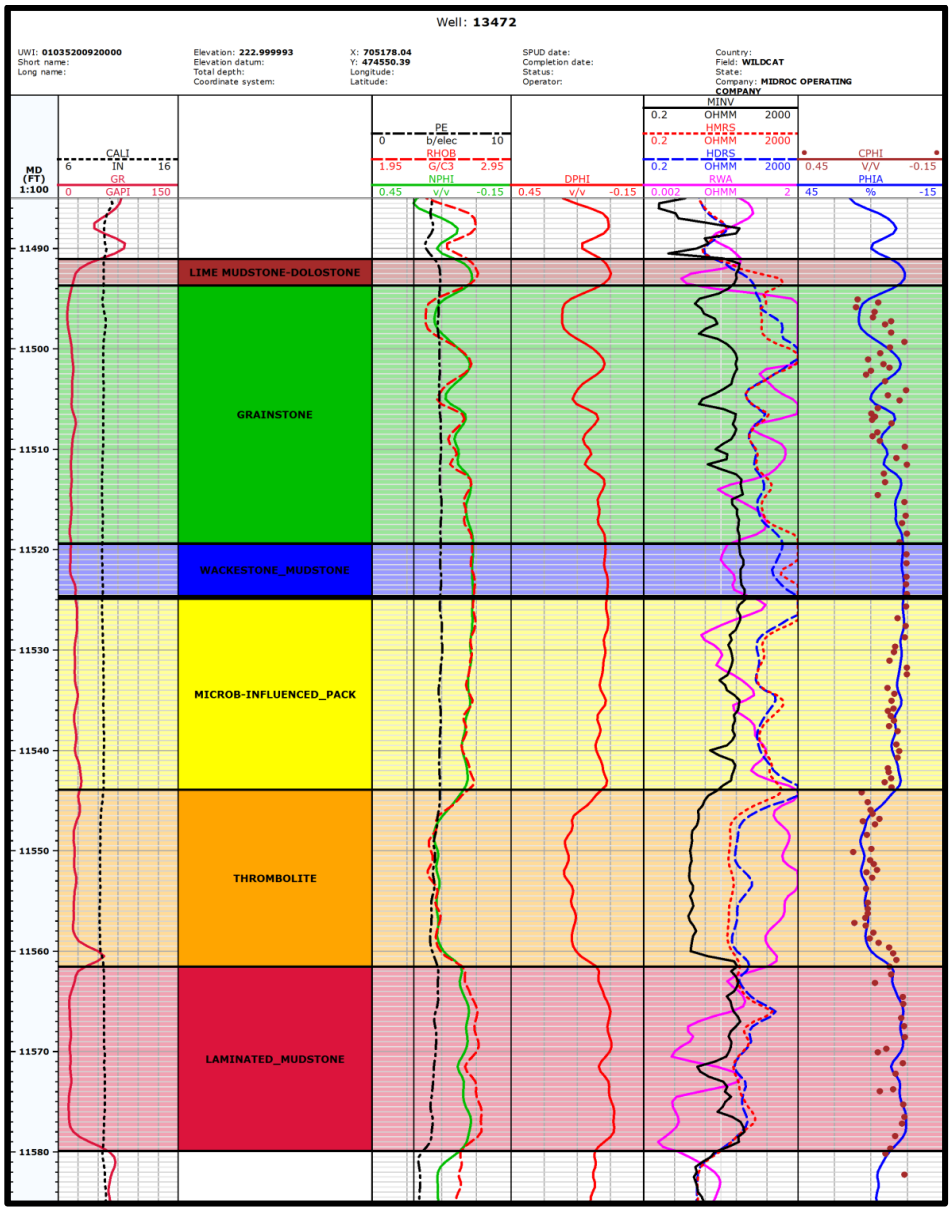

Fig. 13 — Type Log of Smackover Formation in the Little Cedar Creek Field (Al Haddad, 2012).

Petrophysical Model Uncertainty

There are many sources of uncertainty in the Little Cedar Creek Field petrophysical model. With the unavailability of 3-D seismic data, there is no continuity of direct control with the porosity and permeability values in the inter-wells areas; therefore, the predicted vuggy pore types and the associated high permeability in the microbial boundstone reservoir in these areas are highly uncertain. Further, the SGS in combination with collocated cokriging used to model the permeability in inter-well areas requires a simple linear relationship between the statistical parameters (porosity and permeability). In the Little Cedar Creek Field, no simple linear correlation between porosity and permeability is evident (Al Haddad, 2012). Moreover, permeability, whether from the cores or calculated from the logs for 93 of the 113 wells (85%) drilled in the field, was used in predicting the 3-D permeability distribution. In addition, extrapolation of porosity and permeability values in the field, especially in the area of the field boundaries or where no wells exist represents additional uncertainty. The uncertainty in permeability affects reservoir connectivity and pressure gradients, whereas the porosity uncertainty affects the field OOIP and, in turn, the reservoir pressure. The effect of the uncertainty in the petrophysical properties related to the oil flow rate was obvious when running the simulation model.

RESERVOIR ENGINEERING DATA ANALYSIS

Reservoir Fluid Characterization

Five fluid PVT analyses were available for the study: three surface recombination samples from well 10560, 13301, and 13472 and two subsurface samples from well 15263-B and 15731 (Little Cedar Creek Field PVT). Well 10560, 13301, and 15731 are producing from the grainstone-packstone reservoir while well 13472 and 15263-B are producing from the microbial boundstone reservoir. Validation of the PVT samples with production data was required in order to reject unrepresentative sample(s).

Grainstone-Packstone Reservoir Fluid Characterization

The PVT samples (**Table 1**) confirm that the fluid in the grainstone-packstone reservoir is under-saturated conventional black oil. The available PVT samples were validated with early production data and static bottom-hole pressure (BHP) data. The solution-gas oil ratio (R_s) for the three samples was compared to the early producing gas-oil ratio (GOR) of the respective wells. At reservoir pressures above bubble point pressure (P_b), the GOR from producing wells should be equal to or less than R_s by 10-20 % due to venting of the stock-tank gas (The Properties of Petroleum Fluids, second Edition). Well 15731 PVT analysis was rejected because the sampling date was after the inception of gas injection (August 2007). **Fig. 14** and **15** show the producing GOR vs. time for wells 10560 and 13301, respectively. Well 10560 produced at a GOR ≈ 1,000 scf/STB for 5 months while the sample R_s is 522 scf/STB. The disagreement between R_s and early producing GOR was interpreted to be due to the surface recombination sampling procedures. Well 10560 PVT report shows that the separator gas and oil were recombined at 472 scf/STB while the production data shows that the well GOR stabilized around

1,000 scf/STB for almost 5 months. This means the well might not flow long enough to reach its stabilized producing GOR before surface sampling was conducted. With this large difference between well producing GOR and the sample R_s, well 10560 PVT reported was rejected. Also, the well 10560 GOR abnormal behavior is probably attributed to the installation of the ESP pump. With ESP completion configuration, most of wellbore free gas is vented into the annulus and flared; therefore, the measured gas flow rate at the surface becomes less than the actual gas flow rate in around the wellbore. This might explain why the GOR for well 10560 decreases after ESP installation.

TABLE 1—PVT SAMPLES FOR THE GRAINSTONE-PACKSTONE RESERVOIR FLUID

Well	P_b, psi	R_s, scf/STB	Date	* Depth, ft-TVDSS	P_r, psi
10560	1775	522	Dec.-1994	11,582	5388
13301	3030	1074	Sept.-2004	11,366	3664
15731	2220	769	Nov.-08	10,921	4613

• Mid of perforations

The GOR (≈980 scf/STB) for the early production for the well 13301 is in agreement with the R_s (≈1074 scf/STB) reported in the PVT analysis. The static BHP vs. date of production for well 13301 (**Fig. 15**) shows two different slopes: rapid pressure decline for values above 3040 psi and less steep slope for values below 3040 psi. The change in the slope of static BHP vs. time for reservoir producing under solution gas-drive suggests an increase in reservoir compressibility due to the release of gas bubbles. The point where the pressure slope changes is approximately the reservoir fluid bubble point pressure. For well 13301, both P_b in PVT analysis and P_b interpreted from pressure data is in agreement. Therefore, the well 13301 fluid sample is the only valid PVT sample for the grainstone-packstone reservoir fluid, and it was used in this reservoir simulation.

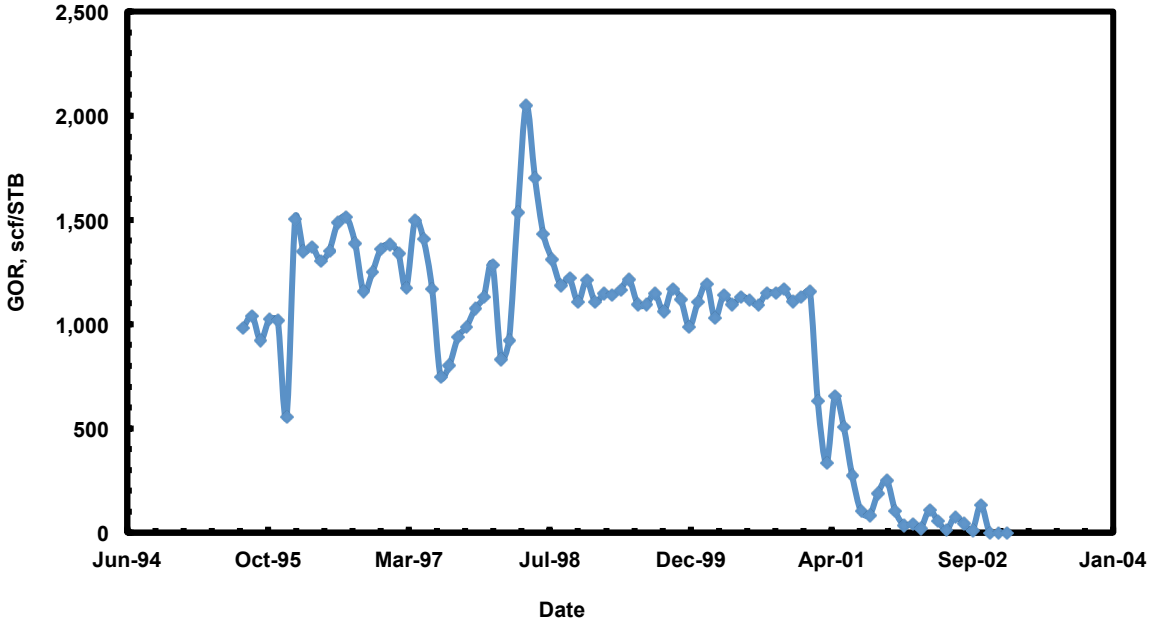

Fig. 14 — Producing GOR for well 10560.

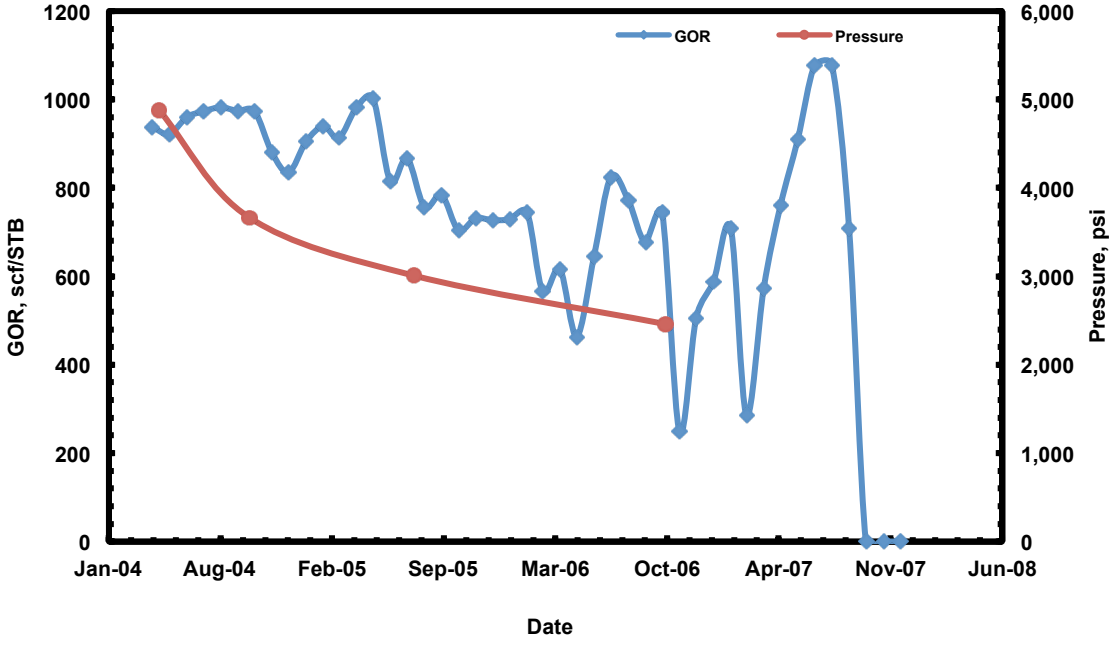

Fig. 15 — Producing GOR and BHP pressure for well 13301.

Microbial Boundstone Reservoir Fluid Characterization

The PVT samples (**Table 2**) confirm that the fluid in the microbial boundstone reservoir is under-saturated conventional black oil. The two available PVT samples were validated with the GOR for the early production (**Figs. 16** and **17**). Again, the abnormal GOR trend for well 13472 is attributed to ESP installation, and subsequent free gas venting into the annulus. The validation shows that the GOR for early production and the laboratory reported R_s for well 13472 and well 15263-B are in agreement; however, the P_b increases with depth while C_{7+} mole fraction decreases with depth (**Fig. 18** and **19),** which is a reversal of what would be expected due to compositional grading**.**

TABLE 2 — PVT SAMPLES FOR THE MICROBIAL BOUNDSTONE RESERVOIR FLUID

Well	P_b, psi	R_s, SCF/STB	Date	* Depth, ft-TVDSS	P_r, psi	C7+, Mole Fraction
13472	3177	945	Sept.-2004	11,322	5066	26.403
15263-B	2640	990	Aug.-2007	10,304	3431	30.469

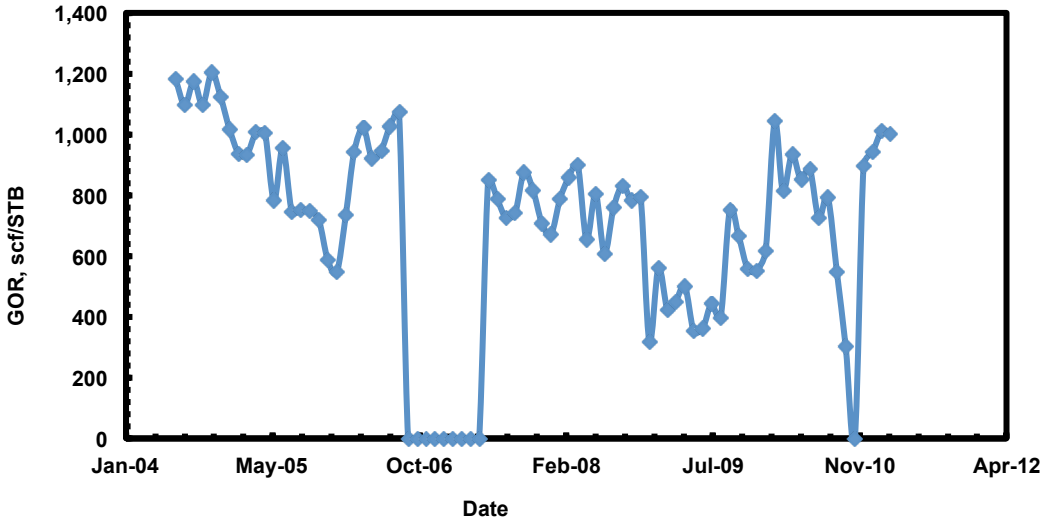

Fig. 16 — Producing GOR for well 13472.

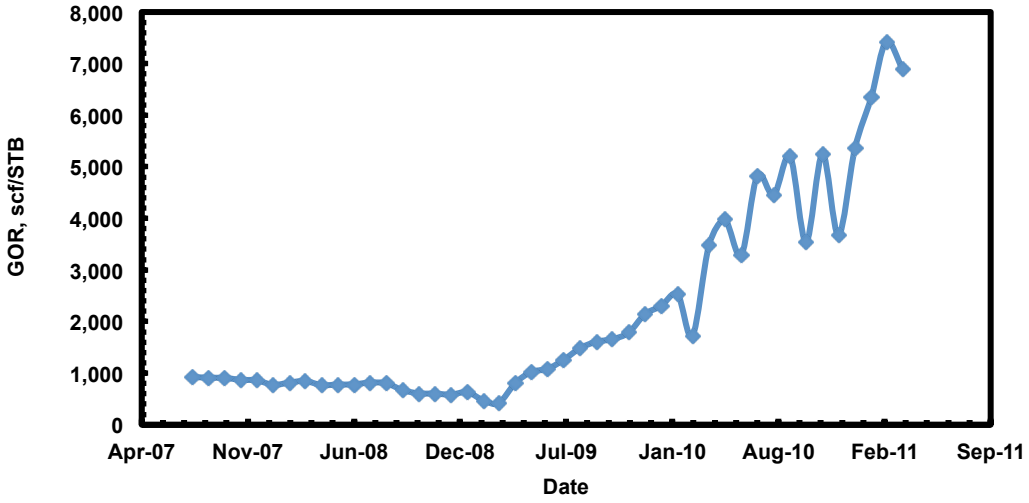

Fig. 17 — Producing GOR for well 15263-B.

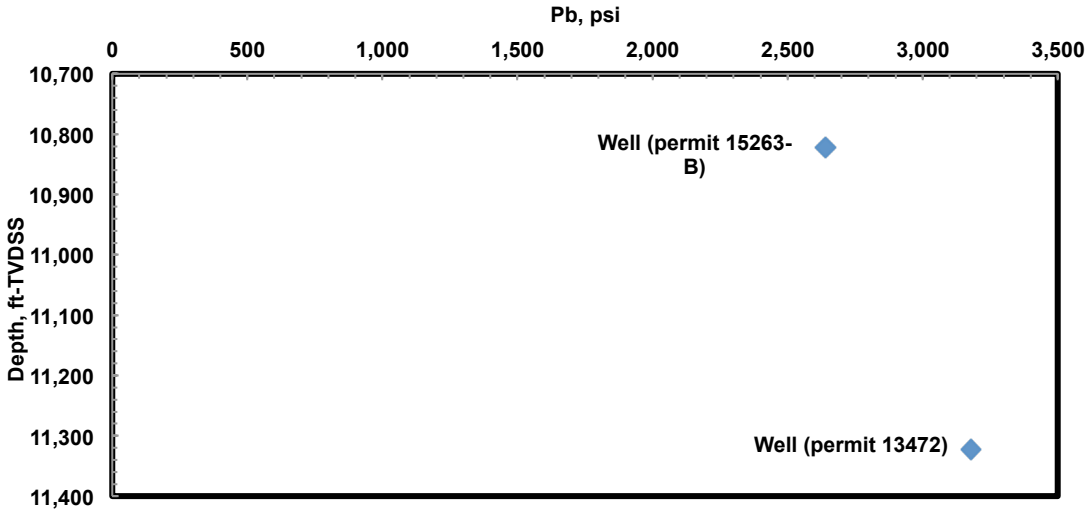

Fig. 18 — Pb vs. depth for the grainstone-packstone reservoir fluid samples.

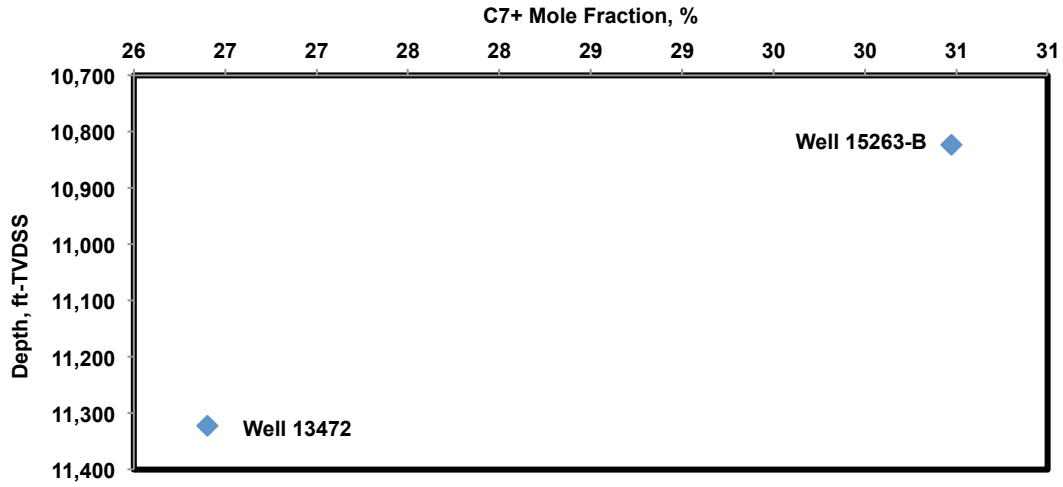

Fig. 19 — C7+ mole fraction vs. depth for the grainstone-packstone reservoir fluid samples.

Since there is no reason to accept or reject one of the two samples, the sample for well 13472 was used in reservoir simulation for the microbial boundstone reservoir. This sample was used because it was obtained earlier than the sample for well 15263-B.

Production Data Analysis

Oil production from the Little Cedar Creek Field started in 1994 when well 10560 was drilled and completed in the grainstone-packstone reservoir (Mancini et al., 2008). The field remained as a single-well field until 2000 when substantial drilling began. The first oil production from the microbial boundstone reservoir was in 2004 when well 13438 was drilled and completed. In August 2007, two wells 12872 and 13301 were converted into gas injectors to inject sweetened, dried natural gas into the grainstone-packstone reservoir for pressure maintenance in the unitized southwestern portion of the field. Out of 73 producing wells in the Little Cedar Creek Field, 23 wells are producing from the grainstone-packstone reservoir only with cumulative oil production of 2.7 MMSTB, 33 wells are producing from the microbial boundstone reservoir only with cumulative oil production of 7.3 MMSTB, and 16 wells are producing from both reservoirs with cumulative oil production of 3.1 MMSTB. The oil production rate for the field reached its peak in January 2009 (**Fig. 20**). Due to the accuracy of reported gas and oil volumes to Geological Survey of Alabama, the field-wide GOR shows anomalous values from March 2001 to August 2003. Except for anomalous GOR values from March 2001 to August 2003, the field-wide GOR remained almost constant, around 1 Mscf/STB until January 2004, when the first oil production came from the microbial boundstone reservoir. The microbial boundstone reservoir fluid has a lower initial solution gas-oil ratio (R_{si}) than the grainstone-packstone reservoir fluid; therefore, the field GOR decreased and remained constant, around 0.9 Mscf/STB. Later, the field GOR slightly decreased and then continue increasing to higher values, indicating one or both reservoirs were producing with pressure below the P_b. The Little Cedar Creek Field water-cut (**Fig. 20**) is very low; it reached its peak (4.3%) in June 2010. The low field-wide water cut indicates that there is no noticeable water encroachment into either one of the reservoirs and supports the conclusion that the Little Cedar Creek Field is producing under solution-gas drive.

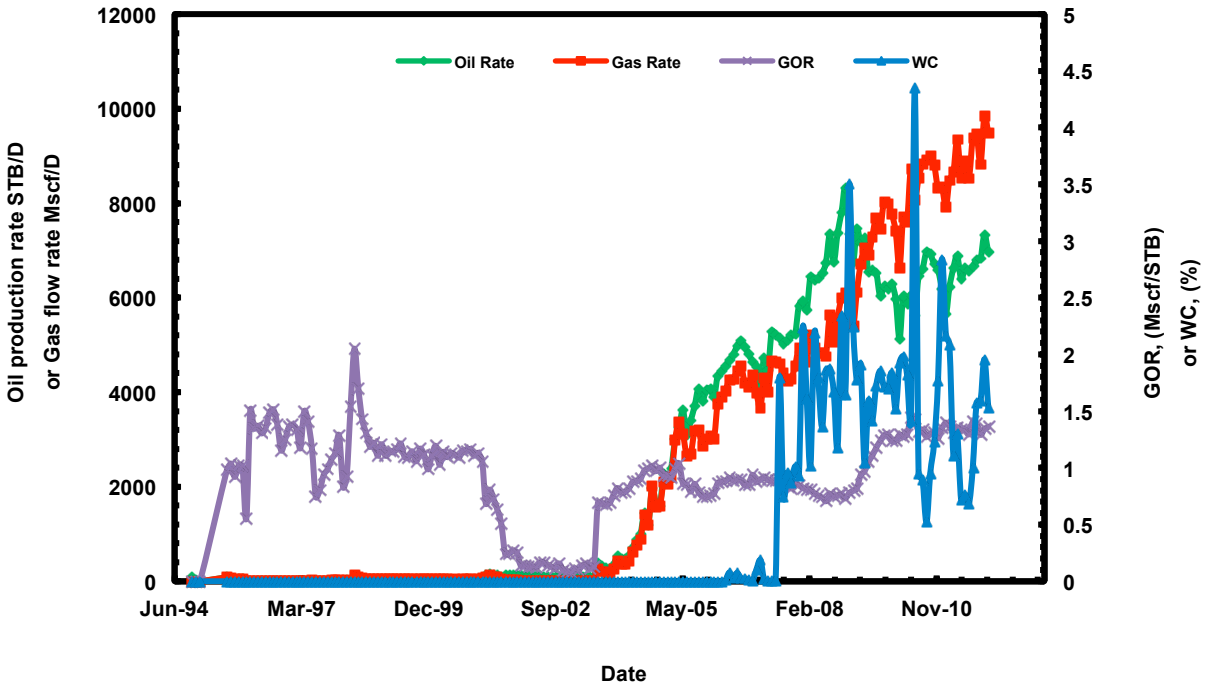

Fig. 20 — The Little Cedar Creek Field production history.

The two wells 12872 and 13301 were converted into injectors to inject gas into the grainstone-packstone reservoir since August 2007. The operator of the Little Cedar Creek Field preferred dispersed gas-injection operations (**Fig. 21**), rather than crestal gas-injection operations where the gas is injected into wells completed in structurally higher positions of the reservoir, for the following reasons:

- The Little Cedar Creek Field has not been totally unitized yet, and the operator decided to inject gas into the unitized portion of the field where these two wells are located.
- The Smackover Formation in the Little Cedar Creek Field has low structural relief (dip angle ≈ 1°); consequently, no noticeable improvement in oil recovery efficiency would be derived from a gravity drainage effect.

- No primary gas cap exists in the Little Cedar Creek Field.
- The southwestern area of the grainstone-packstone reservoir is highly-depleted as it has been producing oil since the discovery of the field in 1994.

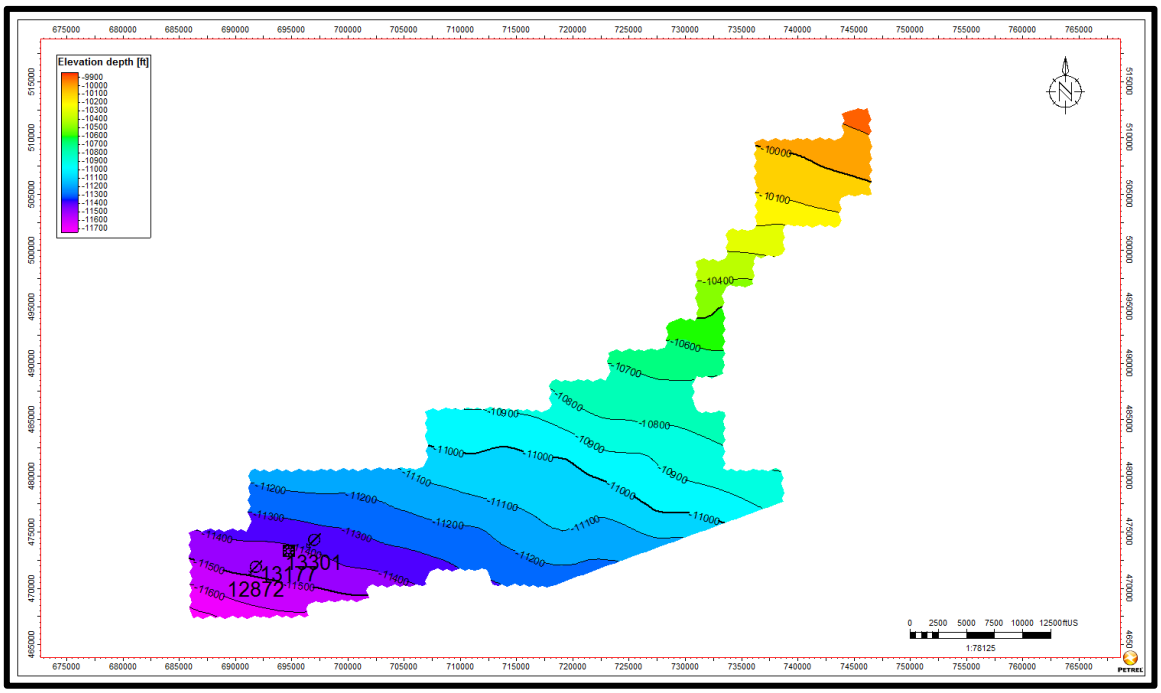

Fig. 21— Structure map (contour interval 100 ft.) on the top of the Smackover Formation in the Little Cedar Creek field showing the locations of the injectors.

Pressure Data Analysis

The Little Cedar Creek Field pressure data are limited. Pressure surveys were not available for all the wells, and most of the available pressure surveys were not measured on a regular basis, and there are no recent pressure survey data were available for this study. The available pressure surveys were quality checked to reject the suspicious values. The pressure surveys available had issues including insufficient shut-in time, unreasonable pressure drop, or the wells were perforated into both reservoirs. **Fig. 22** shows the pressure vs. date for the

grainstone-packstone reservoir. It is difficult to detect any reservoir-wide compartmentalization using these limited data; however, the steep pressure decline rate suggests that there is no other source for pressure support (water drive or gas cap).

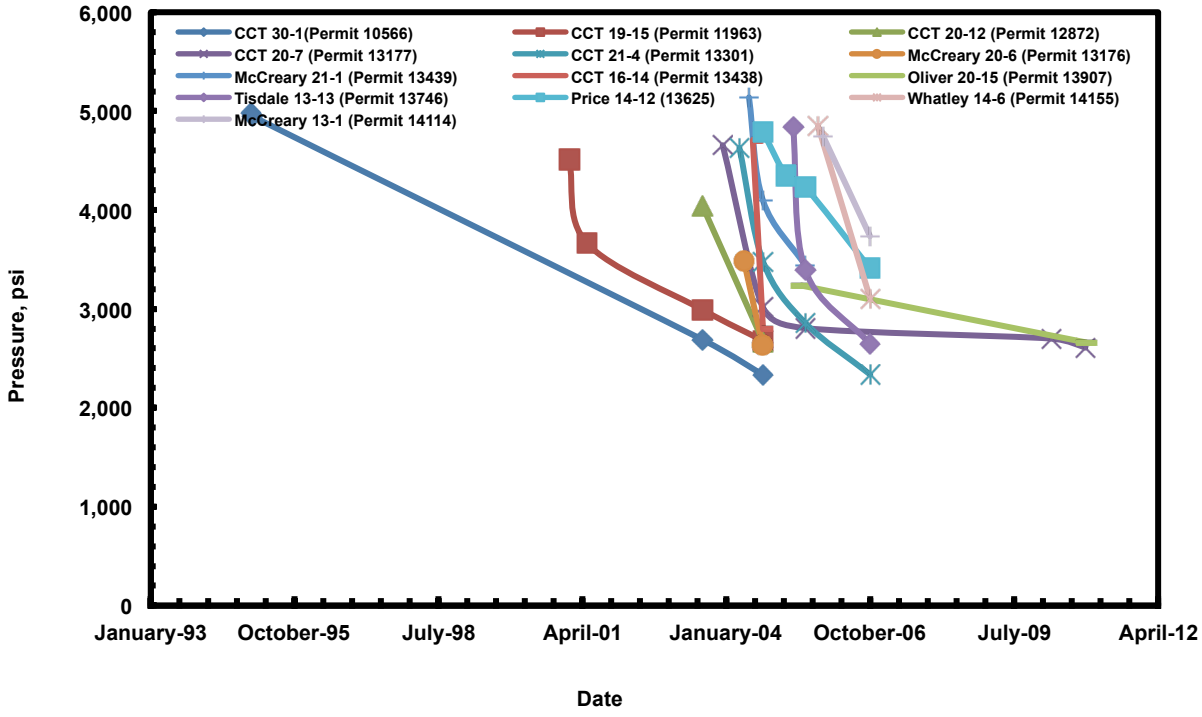

Fig. 22 — The grainstone-packstone reservoir pressure at datum of -10,800 ft.-TVD SS.

Also, the pressure performance of well 13177, which is located between the two injectors, shows that the well responded favorably to the gas injection operation with almost constant static BHP vs. time since the inception of gas injection (**Fig. 22**).

DYNAMIC RESERVOIR SIMULATION

The Schlumberger Eclipse© black oil reservoir simulator was used to generate the 3-D, 3-phase dynamic reservoir model for the Little Cedar Creek field. The 3-D geologic model of Al Haddad (2012) provided the geologic framework for the simulation. Perforation intervals and directional surveys for each well in the Little Cedar Creek Field were obtained. The monthly volumes of produced oil, gas, and water, since the start of production in 1994, were used for this study. Also, the monthly gas injection volumes were available for the study. The produced volumes were reported with varying degrees of accuracy, depending on the phase of production. The oil production volumes are assessed to be the most accurate, while the volumes of produced gas are less accurate. Some wells in the Little Cedar Creek Field have reported monthly gas production of zero or much less than the solution gas-oil ratio. All the wells in the Little Cedar Creek Field were stimulated (acidized) so negative skin factor values are used in the history matching process. The available interpreted pressure transient analysis for two wells in the field provided a guide about the skin factor values. The skin factor values for these two wells are -5 and -4. Appendix 1 shows the two interpreted pressure transient tests.

Stair-step corner point grids were used rather than pillar corner point grids because there is not any structure closure in the Little Cedar Creek Field (e.g. faults). The corner point grids are useful to capture more geologic detail like curvature of microbial buildups. The grids were aligned in the direction of high permeability (70^{o} to the North) to minimize the grid orientation effect (**Fig. 23**) (Reservoir Simulation, SPE Monograph, Vol. 13). The 3-D geocellar model was up-scaled, and the final simulation model uses a corner-point grid system with uniform grid block sizes of about 328 ft in the x-direction and 371 ft in the y-direction and 16 layers. Layer 1 is the peritidal lime mudstone facies. Layers 2-6 are the grainstone-packstone reservoir. Layer 7 is subtidal wackestone facies. Layers 8-10 are the microbially-influenced packstone facies. Layers 11-15 are the microbial boundstone reservoir. Layer 16 is transgressive lime mudstone-

dolostone facies. Excluding the impermeable layers, the simulation model consists of a 65,485 active grid blocks.

Model Initialization

The model was initialized using equilibrium for the oil phase with the OWC set outside the field area because we cannot locate the OWC using the available log data and field WC is low (**Figs. 23** and **24**). The initial reservoir pressures for the upper and the lower reservoir are 4,979 psi and 4,832 psi, respectively, at reservoir datum of 10,800 ft-TVDSS. Due to the unavailability of SCAL data, the relative permeability and capillary pressure were estimated using the Corey correlation and then treated as history matching parameters. Two sets of relative permeability and capillary pressure data were used, one set for each reservoir. This technique allows more flexibility in changing each set independently of the other set

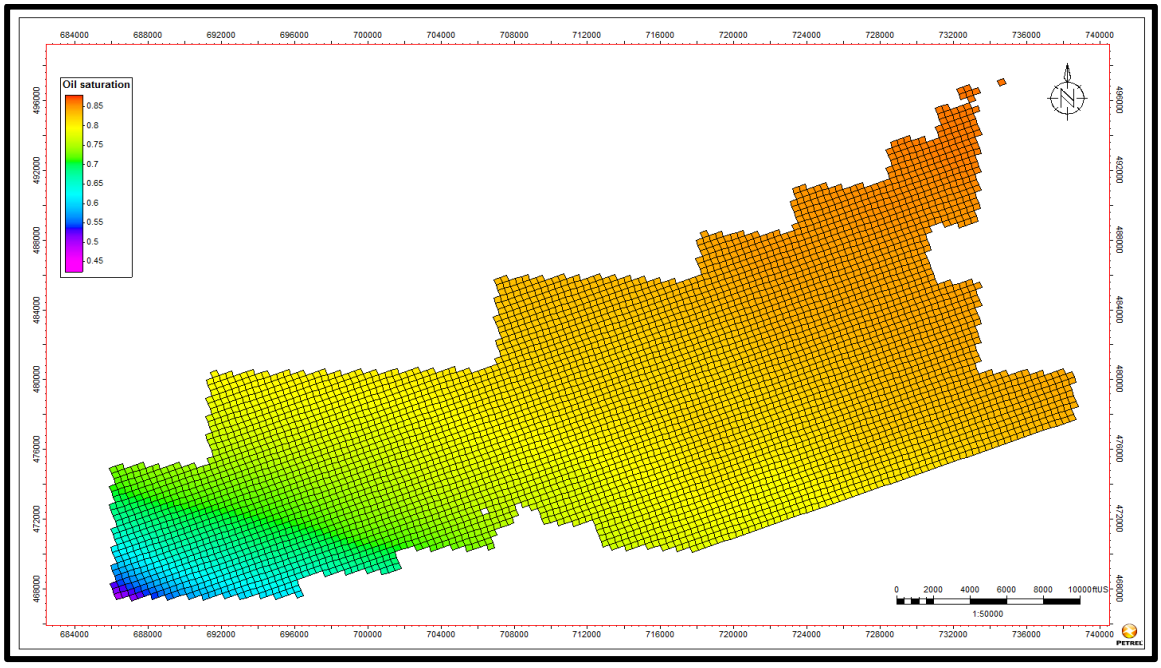

Fig. 23 — Initial oil saturation distribution in the top of zone 2 (the grainstone-packstone reservoir).

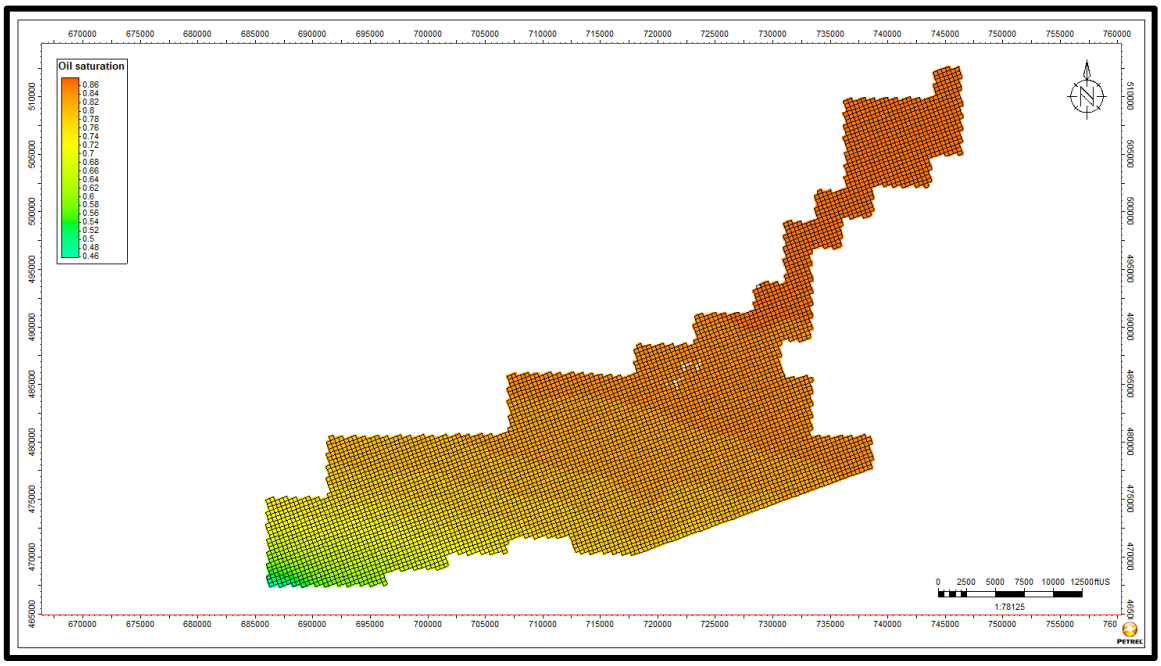

Fig. 24 — Initial oil saturation distribution in the top of zone 11 (the microbial boundstone reservoir).

History Matching

The strategy adapted for history matching of the Little Cedar Creek Field performance involved running the model using the daily oil flow rate as a control, matching the static bottom-hole pressure by well, and then matching the GOR for the field and the key wells. Running the Little Cedar Creek Field simulation model using daily oil flow rate as control was done for two reasons. First, the field-wide water-cut values were too low (**Fig. 20**) to have a considerable effect on the reservoir voidage rate and, consequently, the reservoir pressure .Second, most of the pressure data were available when the average reservoir pressure was above the bubble point pressure; consequently, most produced gas came out of solution and does not affect the reservoir pressure. In the absence of any auxiliary data (e.g. transient pressure data, 4-D seismic), the process of history matching became more challenging and time-consuming. Also,

the uncertainties of the reported volumes of the produced gas represented a challenge in history matching of the GOR for the Little Cedar Creek Field.

In the Little Cedar Creek Field and like most carbonate reservoirs, the reservoir heterogeneity and the resulting variable reservoir connectivity significantly impact the reservoir pressure distribution, creating areas in the reservoir with high pressure communication and areas with restricted pressure communication. In addition, the wells are not evenly spaced across the field, and this results in areas of high depletion in the middle of the field and less depleted areas along the margins of the field. As a result, the pressure values from the static BHP surveys are not representative of the average reservoir pressure; therefore, we cannot adequately assess the quality of the reservoir pressure history matching by comparing the simulated average reservoir pressure from the model with the individual well static BHP tests. Matching the BHP tests by well will yield a more representative assessment of the areal reservoir pressure distribution.

The grainstone-packstone reservoir is under gas injection operation and the microbial boundstone reservoir pressure is below the bubble point pressure; thus, the estimation of gas saturation distribution in the grainstone-packstone reservoir and the microbial boundstone reservoir is important in order to estimate the remaining oil saturation in the reservoirs. To match the GOR for all the producing wells in the Little Cedar Creek Field is not practical. Therefore, the approach selected was first to exclude wells producing with gas lift because the gas production from these wells is not representative of the actual reservoir gas production. Second, I reviewed the distribution of cumulative produced gas for both the upper and lower reservoirs to identify the wells that produced the most gas.

Fig. 25 shows that for wells producing only from the grainstone-packstone reservoir, 99% of gas production from this reservoir is from 13 wells. These 13 wells include 2 wells around the injection wells, which have already experienced gas breakthrough. For wells producing only from the microbial boundstone reservoir, 23 wells produced 90% of the gas. GOR matching for these

wells provides a satisfactory gas saturation distribution in both reservoirs (Bastian et al., 1998**,** **Fig.26**).

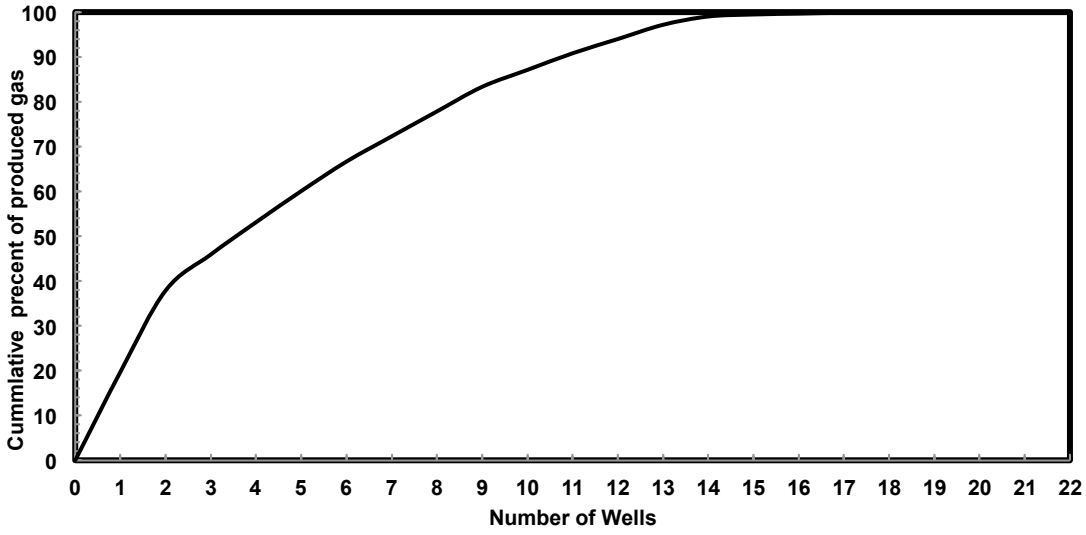

Fig. 25 — Distribution of cumulative gas production vs. number of wells for the grainstone-packstone reservoir.

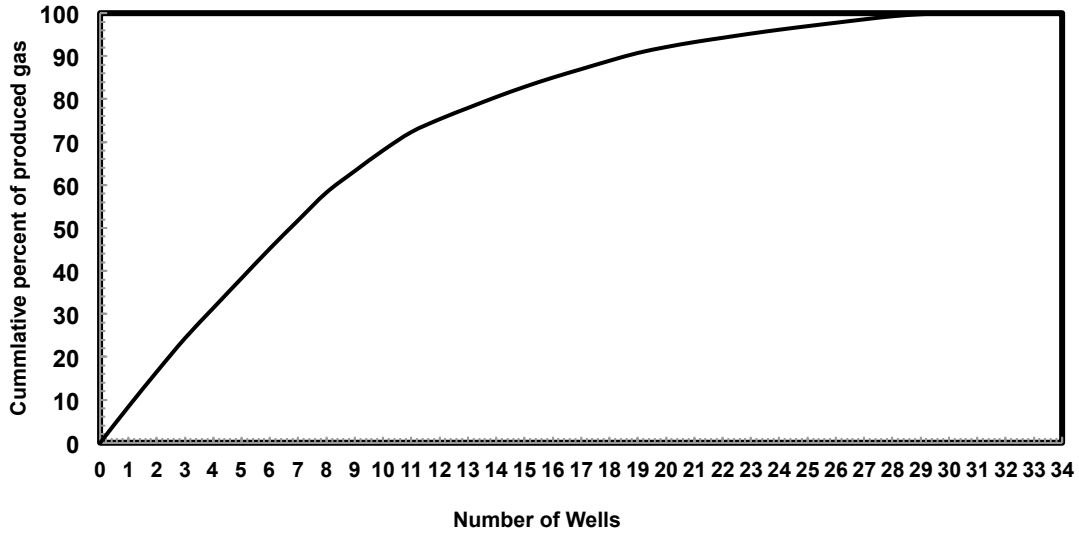

Fig. 26 — Distribution of cumulative gas production vs. number of wells for the microbial boundstone reservoir.

Global changes in the Little Cedar Creek Field model parameters, like oil-water relative permeability; gas-oil relative permeability; and reservoir rock compressibility, have been made to achieve the best possible global performance match. A total of 256 runs with 16 different oil-water relative permeability sets, ranging from a strong oil-wet to a strong water-wet, were tried for each reservoir. Smackover carbonates have been reported to be a strong-water wet system in the Womock Hill Field (Mancini et al., 2004). A strong water-wet relative permeability curve yields the best result for the microbial boundstone reservoir, while a moderate water-wet relative permeability curve yields the best result for the grainstone-packstone reservoir. Also, 25 simulation runs using 5 sets of gas-oil relative permeability, using one set per each reservoir, to provide the best possible model performance match. The reservoir rock compressibility values for both reservoirs were not available for the study; therefore, several correlations were used to calculate the rock compressibility values for both reservoirs. The Hall correlation calculates the rock compressibility as function of porosity and yielded the best global match. A sensitivity analysis was made to assess the influence of reservoir transmissibility (connectivity) and pore volume (**Fig**. **27**) on the reservoir pressure below the bubble point pressure. Changes in pore volume have the greatest effect on the pressure performance in the Little Cedar Creek Field. A pore volume multiplier of 1.2 was applied for the microbial boundstone reservoir as this reservoir is characterized by vuggy pore types, and the 3-D modeling and distributing of this pore types is highly uncertain. The modeled vuggy pore types are believed to be underestimated, especially in the absence of 3-D seismic data (Al Haddad 2012). These above-mentioned changes enhance the history match for GOR and pressures globally.

Local changes in porosity and permeability (increase or decrease) within each well window were done to match well-by-well static BHP data and GOR for key wells. These changes included increasing the permeability values between the injectors and the wells with gas breakthrough. The static BHP data for wells were matched with varying degrees of success. **Figs. 28**, **29**, and **30** show examples of good and acceptable pressure match for wells producing

from the microbial boundstone reservoir, for both reservoirs, and for the grainstone-packstone reservoir, respectively.

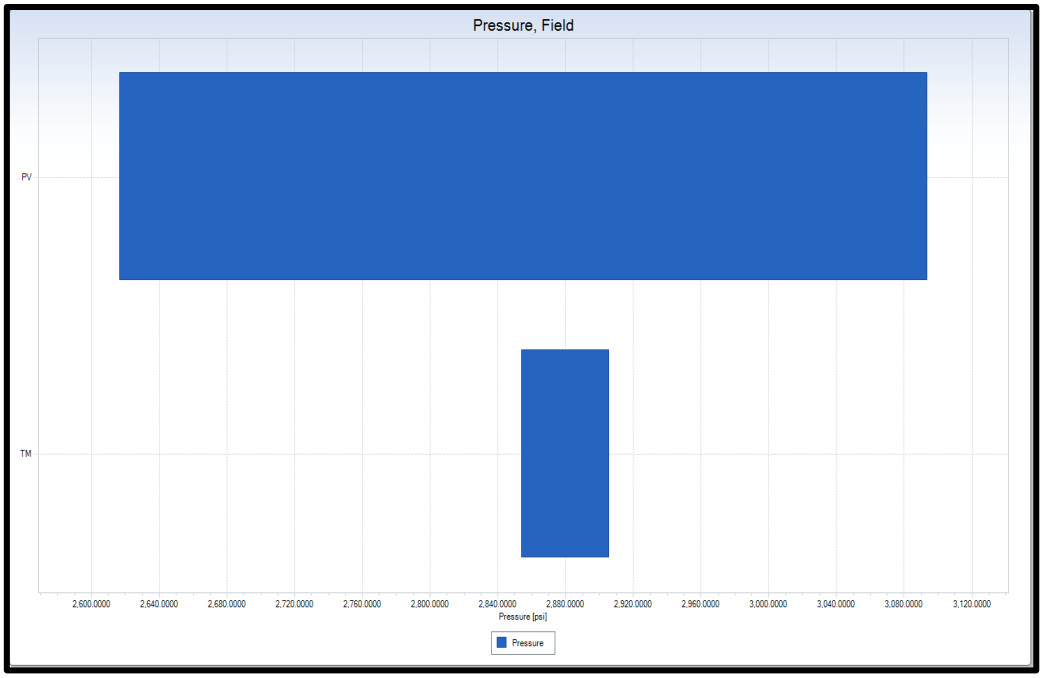

Fig. 27 — Tornado plot for effect of pore volume (PV) and transmissibility (TM) changes on the reservoir pressure.

The Little Cedar Creek Field history matching was the most challenging task of the project, because of the difficulties in the pressure history matching due to limited available data and the uncertainty in the reporting of gas flow rates for some wells. High quality history match is never expected to be achieved with the limited static BHP data.

The history matches of available static BHP are acceptable **Figs. 28**, **29**, and **30**; however, the BHP data are not available for most wells and recent BHP data is available and this, in turn, affects the quality of other performance match. The overall quality of field-wide GOR history match is poor. The accuracy of the reported gas volume affects the quality of gas history matching. Above the bubble point pressure, the GOR should be equal to the solution gas-oil ratio. This is not the case in the Little Cedar Creek Field. The field was producing at a GOR of

less than the reported solution GOR since 2001.This may be attributed to the reported produced gas volumes being less than the actual. The reported produced volumes of oil and gas were downloaded from Geological Survey of Alabama website. Also, from March 2001 to August 2003, the reported GOR was apparently reported as too low (≈ 0.2 Mscf/STB). The GOR was matched for individual wells with varying degree of success. **Fig. 31** shows the GOR history match for well 14069-B producing from the microbial boundstone reservoir, and **Fig. 32** shows the GOR history match for well 14270 with gas breakthrough, and **Fig.33** shows the GOR history match for well 14069-B.

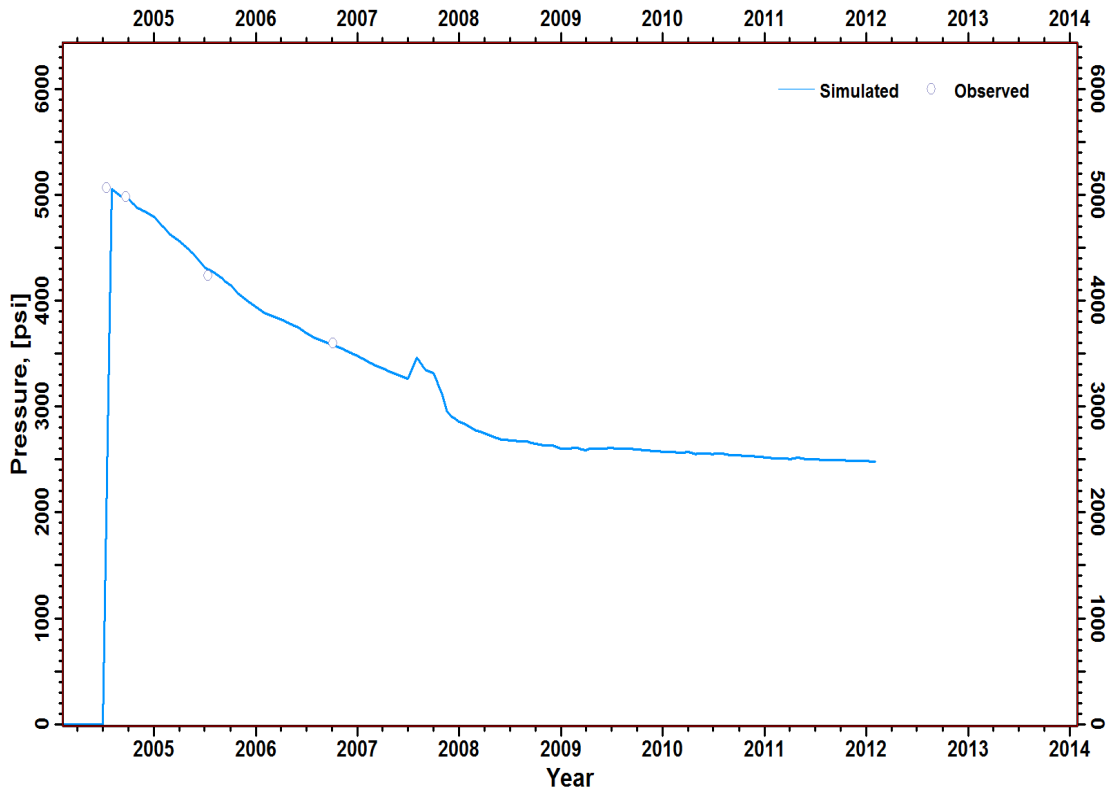

Fig. 28 — Pressure history match for well 13472 (microbial boundstone reservoir).

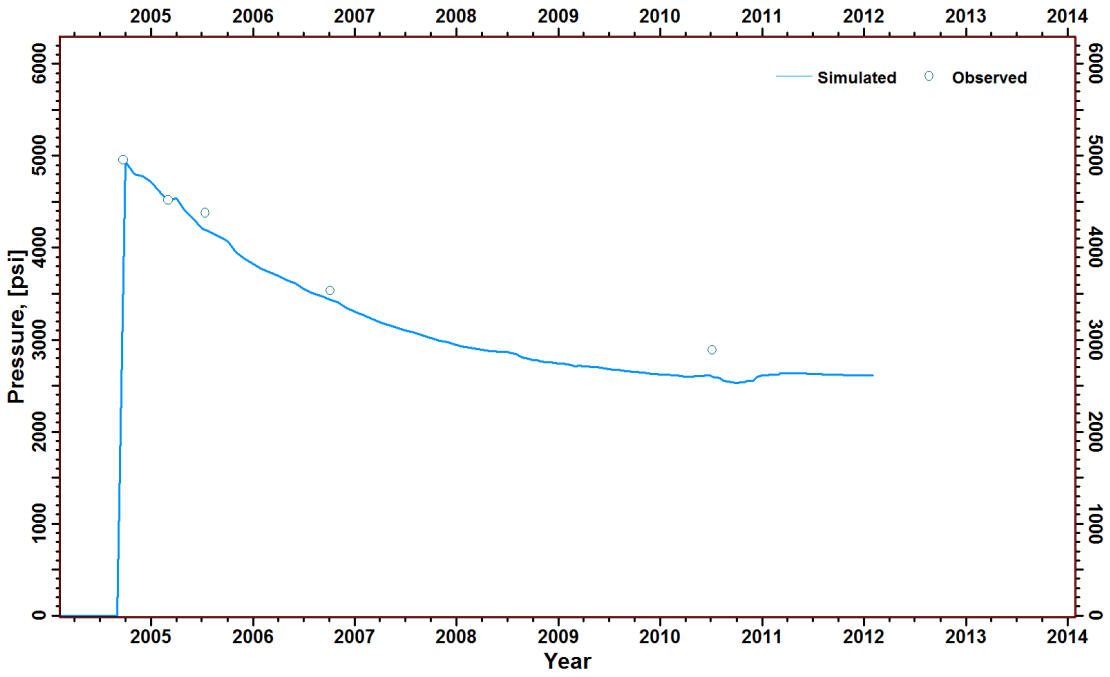

Fig. 29 — Pressure history match for well 13625 (both reservoir).

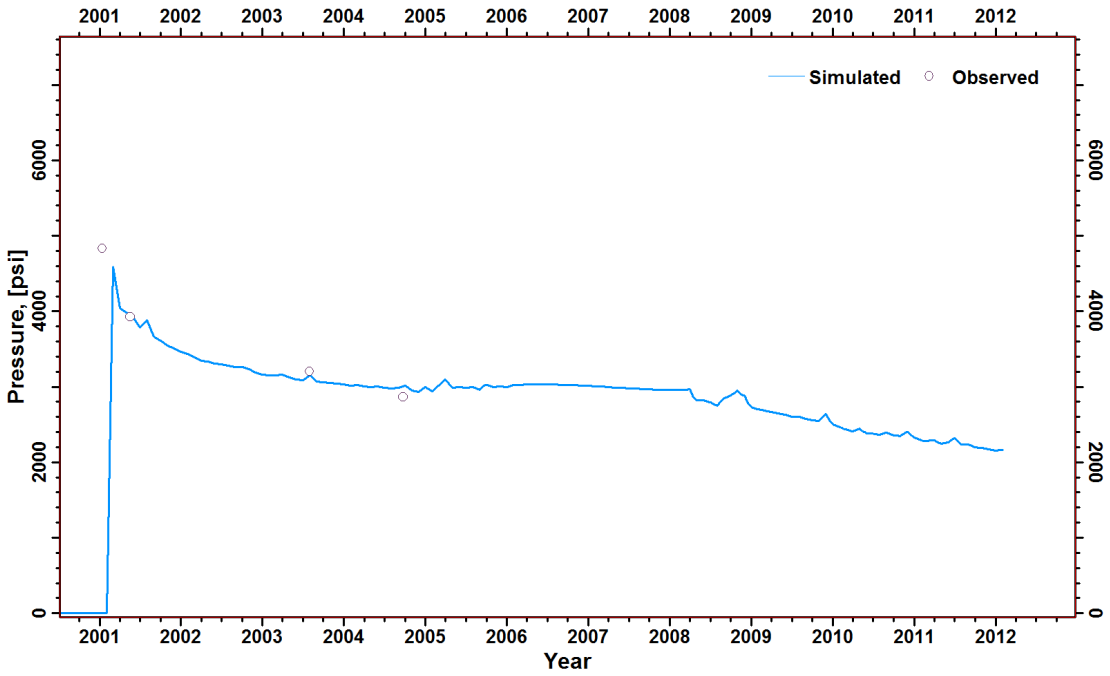

Fig. 30 — Pressure history match for well 11963 (grainstone-packstone reservoir).

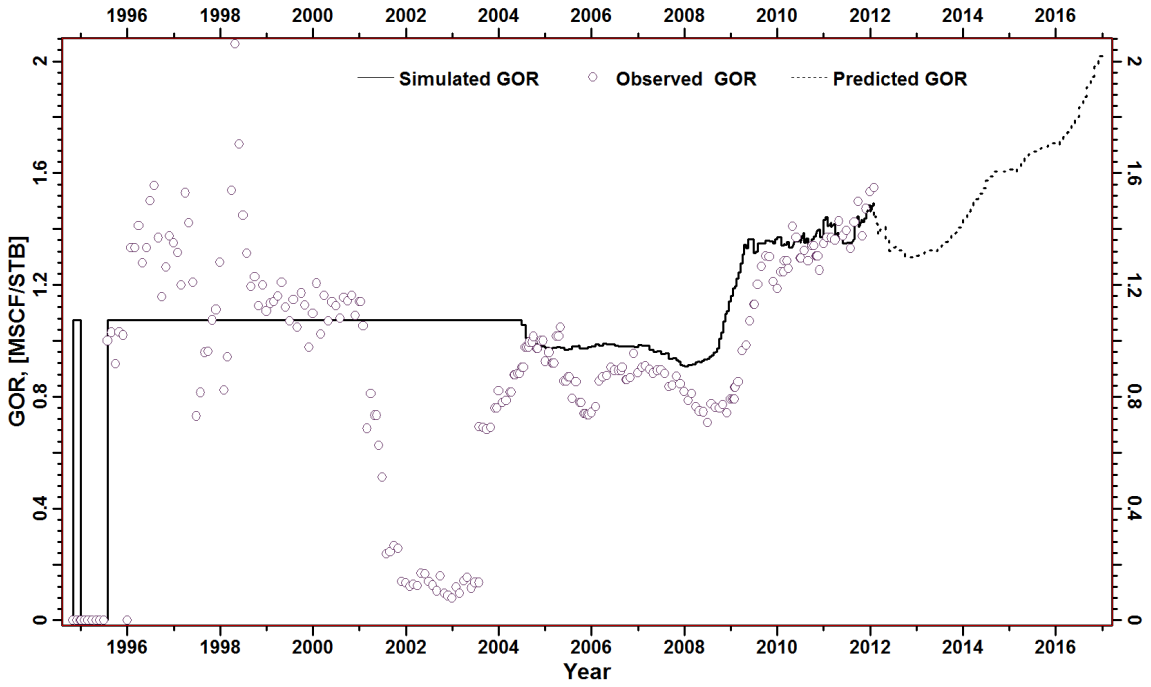

Fig. 31 — The Little Cedar Creek field GOR history match and prediction.

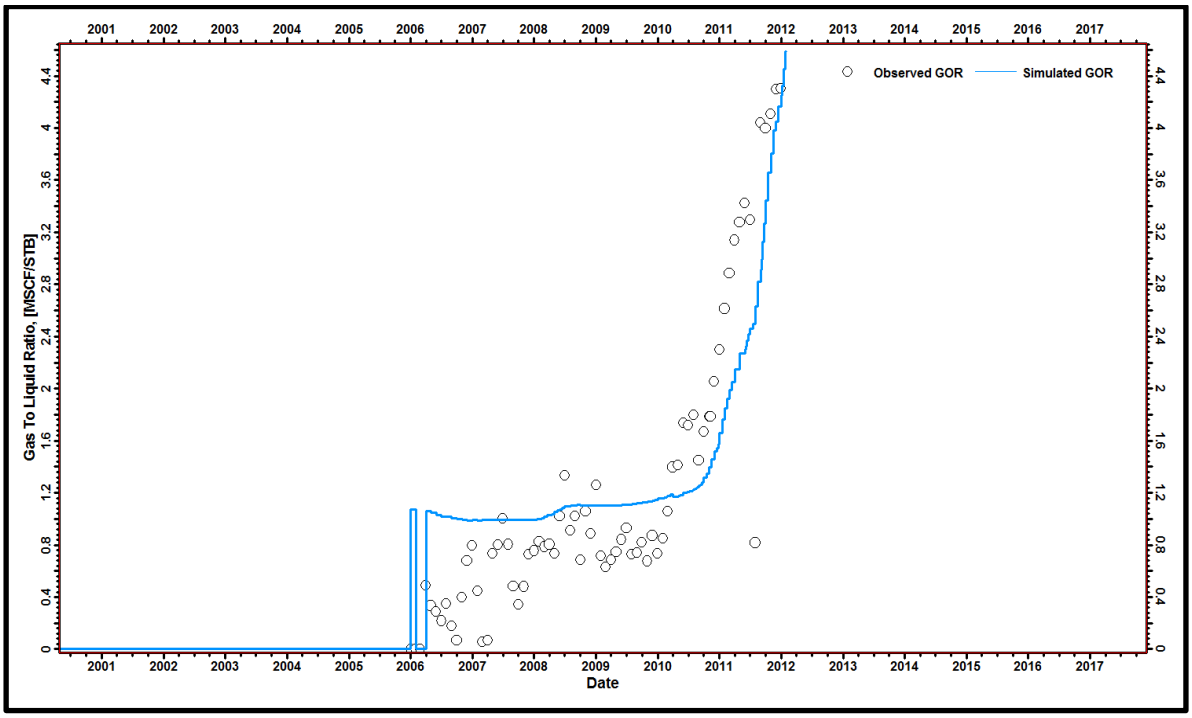

Fig. 32— GOR history match for well 14270.

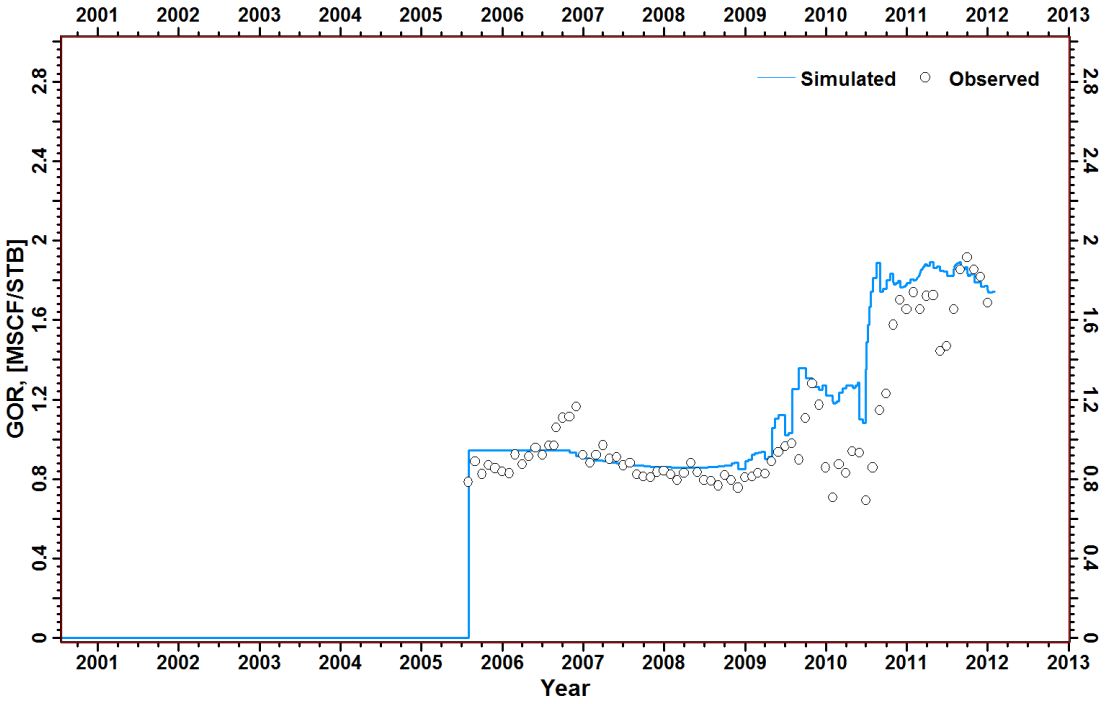

Fig. 33— GOR history match for well 14069-B.

Little Cedar Creek Field Redevelopment Plan

The base case prediction, using bottom hole pressure as control for 5 years starting in January 2012, indicates that oil recovery from the Little Cedar Creek field by January 2017 will be 16.8 MMSTB (**Fig. 34**), which is 18.6% of OOIP (90 MMSTB). A redevelopment plan is required to increase the oil recovery from the field.

With two reservoirs and several layers in each reservoir, the investigation of several development plans will be difficult. The Movable Hydrocarbon Pore Volume (MHPV) was the criteria to identify the potential areas of the field where potential uncontacted oil remains for recovery through drilling and/or improved recovery methods. The MHPV is calculated with:

$$MHPV = \frac{43560\, V_p(S_o - S_{or})}{\Delta X \Delta Y B_o} \qquad (2)$$

where,

B_o = oil formation volume factor, RB/STB

S_o = oil saturation, fraction

S_{or} = residual oil saturation, fraction

V_p = pore volume of a simulation grid block, RB

ΔX = x-dimension of simulation grid block, ft

ΔY = y-dimension of simulation grid block, ft

MHPV has several advantages. This approach provides a direct measure of the amount of recoverable oil because it is a volumetric calculation. Also, it represents the movable oil that can be affected by water or gas injection. An MHPV map for each layer at the end of the history match along with the permeability maps were used to select the proposed well locations. Appendix 1 shows bottom-hole coordinates and perforation intervals for proposed new wells to be drilled, identifies wells to be entered to drill side tracked wells, and also shows the proposed

work-over wells. **Fig. 34** shows the predicted oil recovery after implementation of the improved development plan while **Fig. 31** shows the predicted GOR associated with the redevelopment plan.

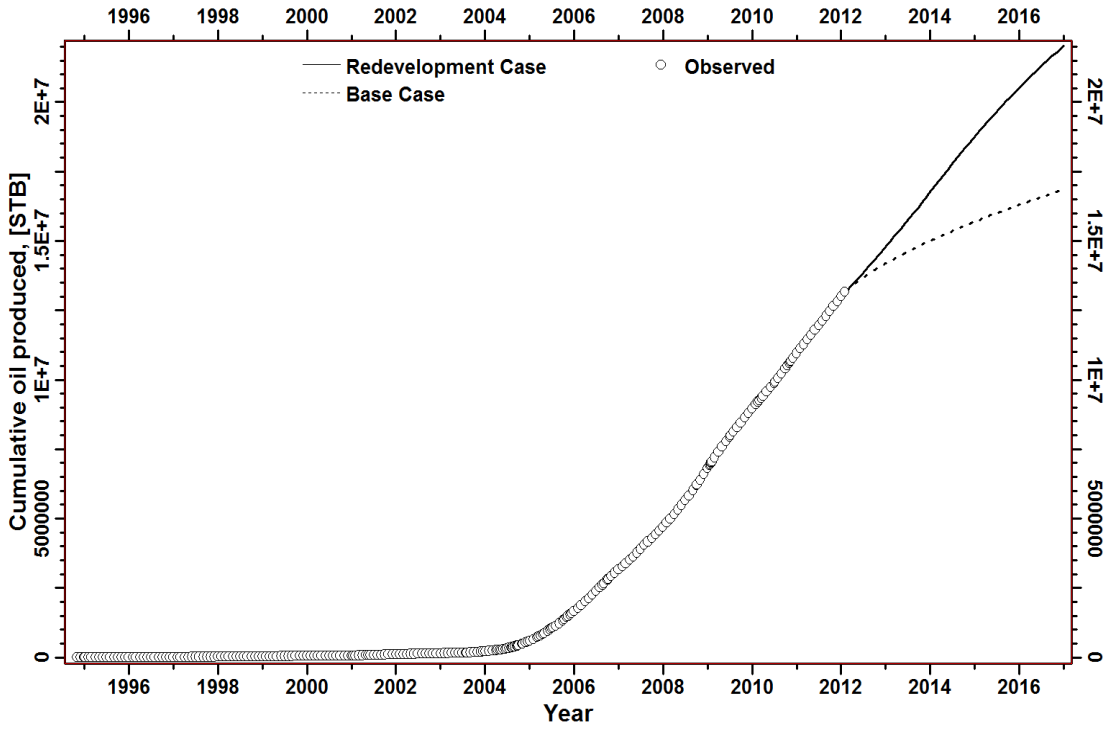

Fig. 34 — Base case prediction vs. redevelopment plan.

Redevelopment Plan of the Grainstone-Packstone Reservoir

The 5-year redevelopment plan for the grainstone-packstone reservoir involves converting a third well 13583 into gas injector, drilling 7 new wells maintaining 160-acre unit size, side tracking 1 well, and initiating work-over operations on 3 wells. Using the MHPV and permeability maps, I proposed locations for drilling these 7 new wells. **Fig. 35** shows the

proposed locations for the 7 wells on the MHPV maps (Prod-G-1, Prod-G-2, Prod-G-3, Prod-G-4, Prod-G-5, Prod-G-6, and Prod-G-7).

The MHPV map shows high remaining recoverable oil in the southwestern portion of the field in the grainstone-packstone reservoir. The occurrence of this oil may be attributed to the displacement effect of gas injection operations (**Fig. 28**). The field southwestern area is considered a target area for further development drilling. **Fig. 36** shows the performance of a well completed in this area.

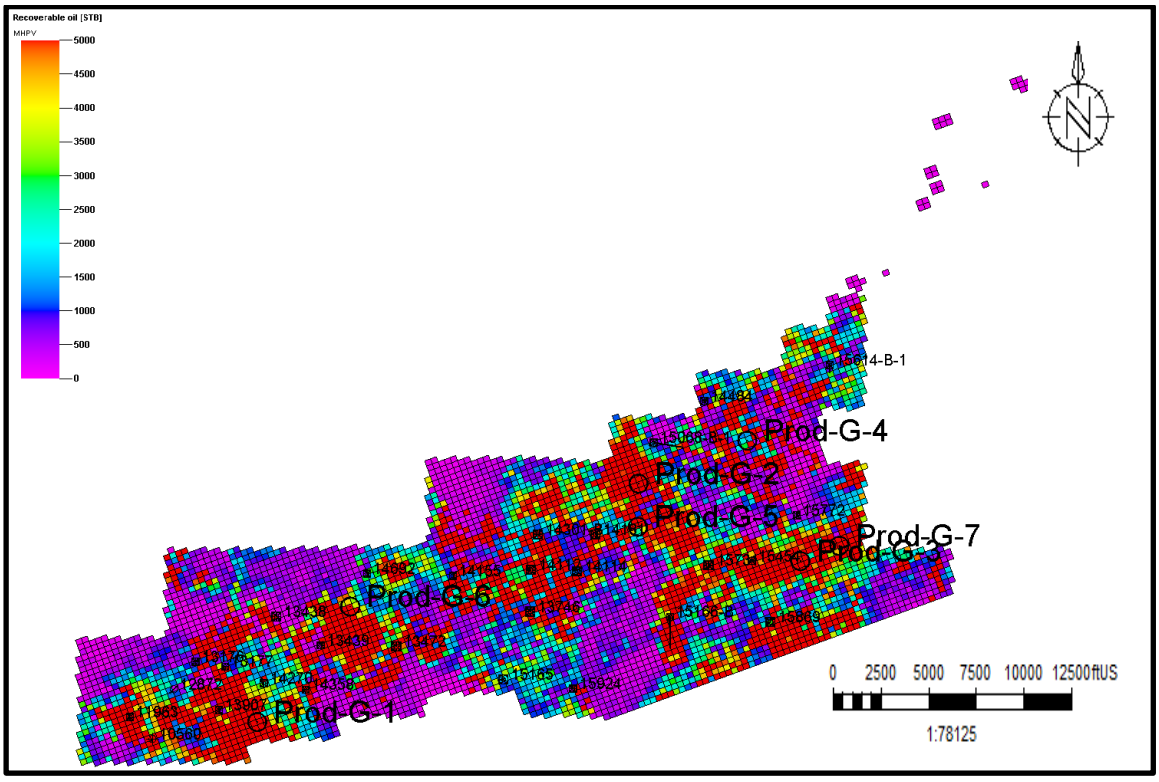

Fig. 35 – MHPV with some wells in the top of zone 2 (grainstone-packstone reservoir) at the end of history matching.

Because of the characteristics of the grainstone-packstone reservoir, including facies heterogeneity (grainstone vs. packstone), pore types (interparticle, moldic), and relatively low permeability, the current well spacing is not efficient to recover all recoverable oil in the field.

This can be seen by the remaining recoverable oil in the inter-areas of drilled wells (**Fig. 35**). More oil can be recovered from the grainstone-packstone reservoir by drilling infill wells (unit size less than 160-acre). Drilling of these infill wells will require unitization of the field.

The 3 wells identified for work-over are candidates for the installation of artificial lift, such as gas lift or ESP, or changing the existing configuration so the wells can be produced. Because the static BHP of these wells is high (4000-3000) psi it is interpreted that there is a considerable fluid column in the well bore of these wells and installing a pump or lowering the already existing pump intake will result in resuming the oil production from these wells. **Fig. 37** shows the performance of well 15068-B-1 before the work-over and the predicted performance after the work-over.

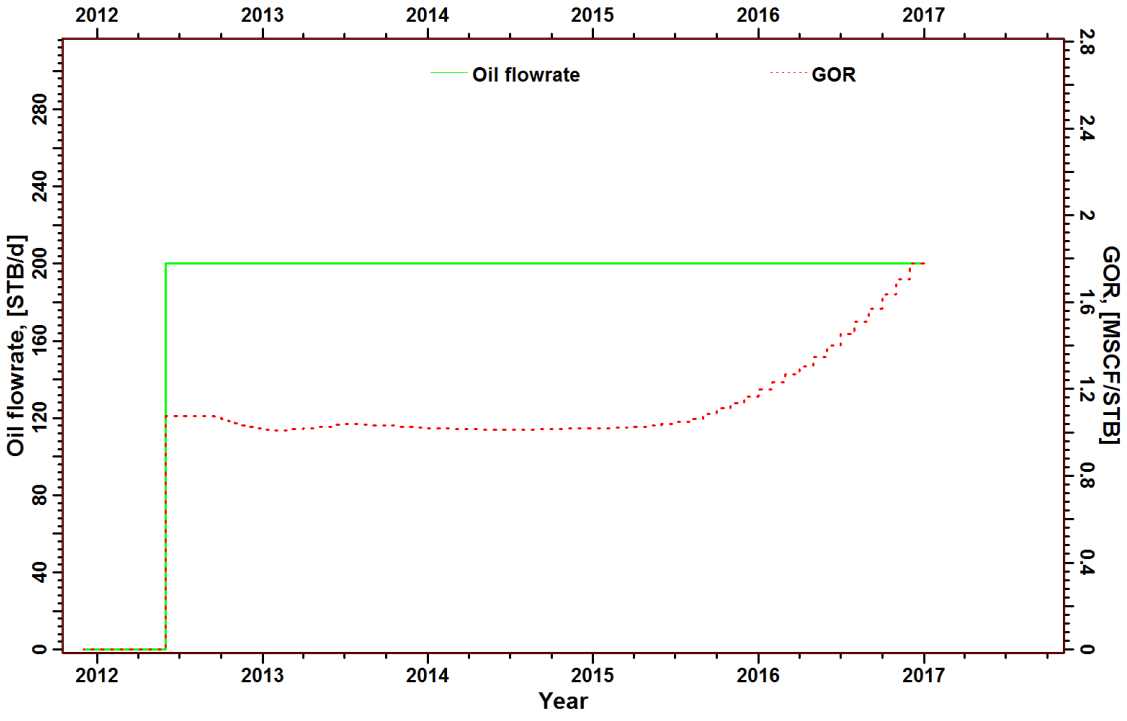

Fig. 36 — Well Prod-G-1 predicted performance.

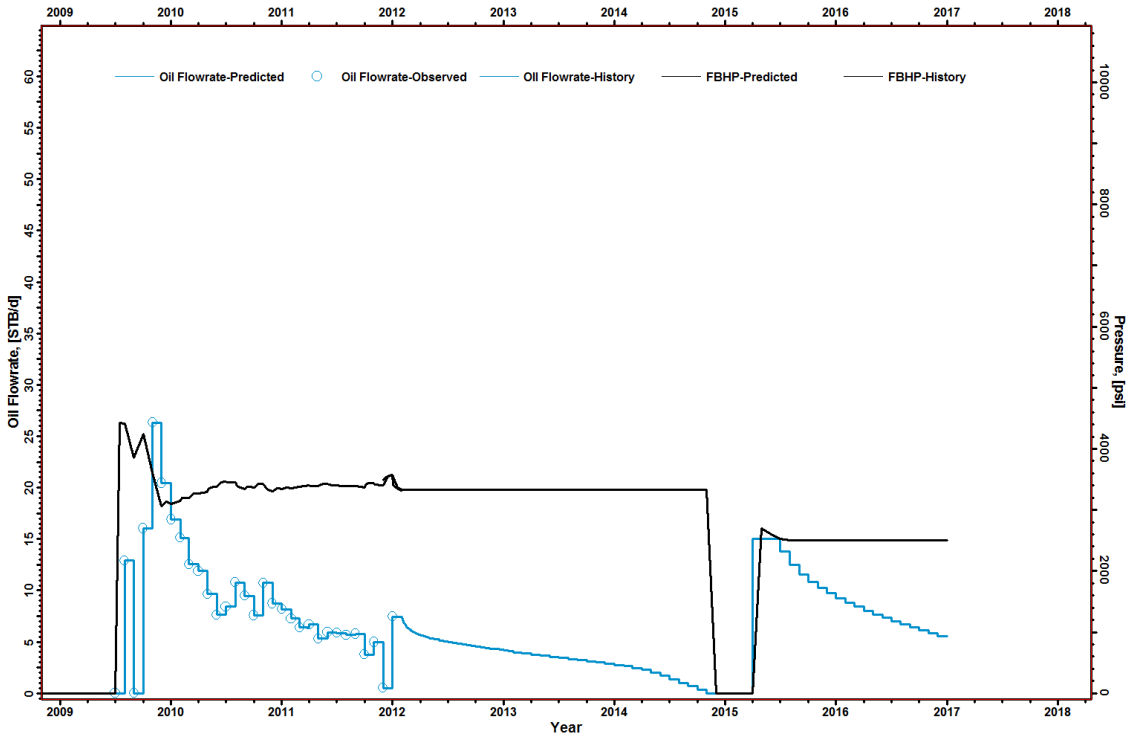

Fig. 37— Well 15068-B-1 performance before and after work-over.

Redevelopment Plan of the Microbial Boundstone Reservoir

The redevelopment plan for the lower reservoir includes drilling 5 new wells, and working-over 16 wells. The reservoir engineering data analysis and simulation studies for the Little Cedar Creek Field indicate that the primary drive mechanism for the field is solution-gas drive. The pressure history and producing GOR indicate that the microbial boundstone reservoir pressure is below bubble point pressure, making it a suitable candidate for secondary-recovery operations. Water-injection is preferred rather than gas injection as a pressure-maintenance operation for the microbial boundstone reservoir in the Little Cedar Creek Field for the following reasons:

1- Free gas exists in the microbial boundstone reservoir as of January 2012; consequently, early gas breakthrough is expected if gas is injected into the reservoir because the gas

saturation is higher than critical saturation. No flood front is expected to be formed in the presence of free gas in the reservoir.

2- Vuggy pore types and associated high permeability zones will also result in earlier gas breakthrough and lessen the areal sweep efficiency since the gas mobility is higher than the oil mobility.

3- Holmgren et al. (1951), Dykstra et al. (1950), Dyes et al. (1954) and Kytle et al. (1956) reported the beneficial effect of free gas saturation in decreasing residual oil saturation left after water injection.

Also, Little Cedar Creek Field simulation studies predict that water injection will result in higher oil recovery in this field compared to gas injection. The comparison study involved simulating the effect of water and gas injection operations independently, and using the same 3 injectors for both water and gas (**Fig. 39**). A 10-year forecast was run to detect the long term effect of the injection operation on the field production rate. In the Little Cedar Creek Field, water injection could result in a higher oil recovery than gas injection by January 2022, with the field oil flow rate remaining the same at the end of the prediction (January 2022) for both cases. Water injection is projected to recover an incremental 1 MMSTB of oil from the microbial boundstone compared to gas injection operations (**Fig. 38**).

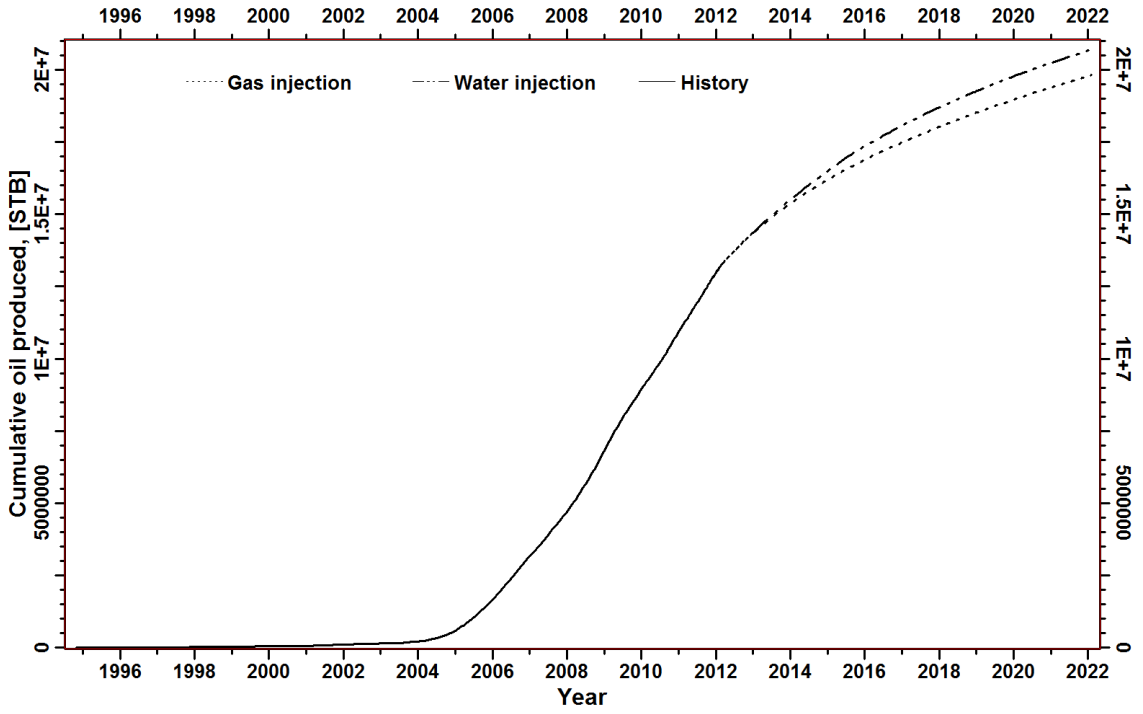

Fig. 38 — Predicted cumulative oil production from the microbial boundstone reservoir for gas injection and water injection.

The selection of water injector locations in the Little Cedar Creek Field does not depend on structural positions as the dip of Smackover Formation beds in the field (≈ 1^{o}) is so slight that it has no significant effect on the selection of the location of the water injection wells. Therefore, other criteria were considered in selecting the location of the injection wells. The locations were selected to avoid extremely high or low permeability zones. The extremely high permeability zones adversely impact the water areal sweep efficiency, whereas the low permeability zones limit the maximum injection rate. Also, reservoir connectivity and potential compartmentalization were considered. The location of the injectors was selected to affect the maximum possible area of the reservoir. Also, the highly depleted areas in the field, where most of production came from, were targeted. Finally, wells shut-in or wells with a low oil production rate received priority for conversion to injectors for economic reasons.

The proposed injection pattern is an external pattern with the injectors located along the edge of the reservoir (**Fig. 39**). The highly depleted and productive area in the middle of the field where the microbial boundstone reservoir is well developed and the areas distant from the low permeability barrier, which separate the southwestern part of the field from the middle part of the field, were targeted areas. The 5-year plan involves converting 3 wells 15165, 14652, and 14740-B-1 into water injectors. Well 15165 is already shut in and perforated into the upper and lower reservoir; the upper perforations must be squeezed in order to direct all the water into the lower reservoir. Wells 14652 and 14740-B-1 are producing at a low rates (≈5 STB/d).

The water injection rate sensitivity analysis using the simulation model showed there is a correlation between the water injection rate and cumulative oil recovered from the Little Cedar Creek field. As the water injection rate increases, the cumulative oil recovered increases. Sensitivity analysis was performed using water injection rate ranging from 600 STB/d to 1200 STB/D per each well of the three injectors. The cumulative recovered oil responded favorably with injection rate increase (**Fig. 40**).

Permeability varies from one layer of the reservoir to the other. To ensure good vertical sweep efficiency of water and uniform distribution of water into the all reservoir layers, the injectors were selectively perforated into layers such as that each layer has two injectors that perforate it. **Fig. 41** to **Fig. 45** shows the water saturation distribution in each layer of the lower reservoir by January 2017. An almost equal area in each layer has been swept by water as result. This proves the effectiveness of a selective perforation technique. Appendix 1 contains the details about the perforation intervals.

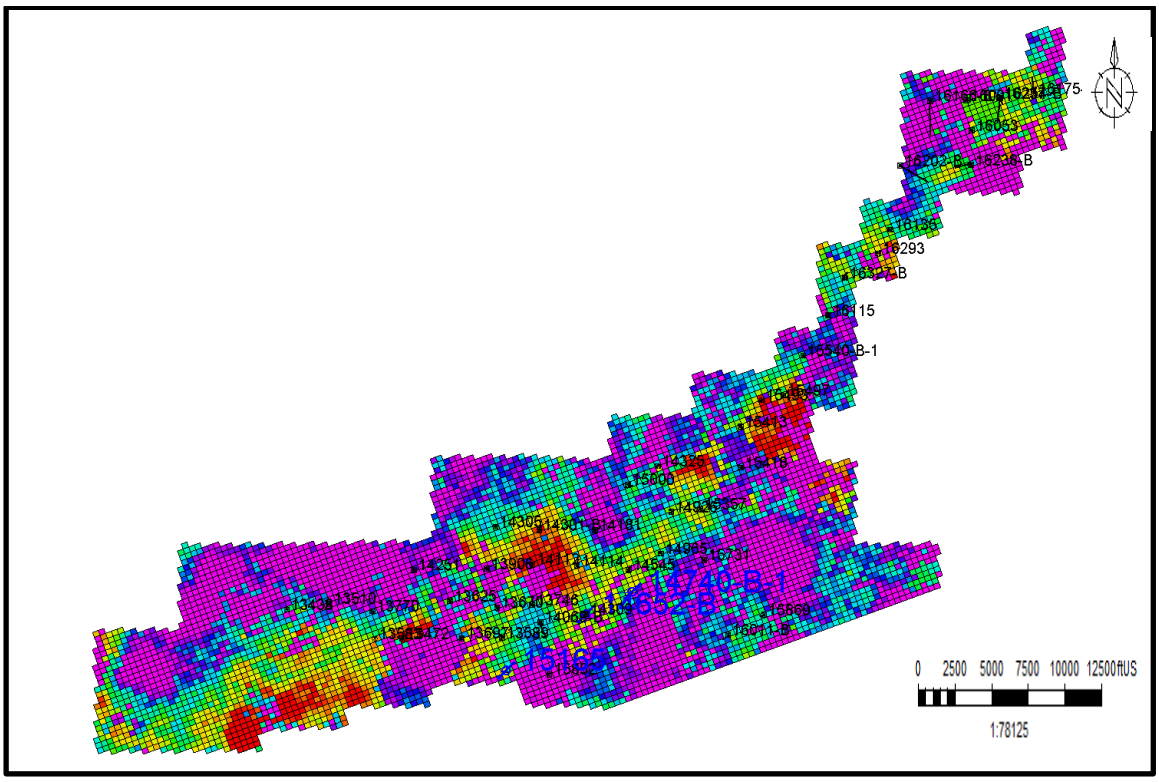

Fig. 39 — Permeability map in the top of zone11 (microbial boundstone reservoir) showing the location of the injectors.

Using the permeability and MHPV maps, 5 locations for potential drilling are identified. These new wells are Prod-M-1, Prod-M-2, Prod-M-3, Prod-M-4, and Prod-M-5 (**Figs.46-49**). The MHPV maps show that high recoverable oil saturation remains in the southwestern portion of the microbial boundstone reservoir. This area is considered promising for any future drilling. MHPV maps show that the remaining oil saturation is less in zone 15 (last zone in the microbial boundstone reservoir) as the transgressive lime mudstone-dolostone facies (lower seal) is more dominant (**Fig. 49**). Unlike the grainstone-packstone reservoir, the microbial boundstone reservoir has less remaining oil saturation in the inter-wells areas; therefore, infill drilling will not result in recovering considerably more oil from this reservoir. The predicted performance of a proposed new well is shown in **Fig. 50**. Also, 16 wells are candidates for work-overs. **Fig. 51**

shows the performance of well 15068-B-1 before the work-over and the predicted performance after the work-over. Appendix 1 shows the work-over operations time for each well.

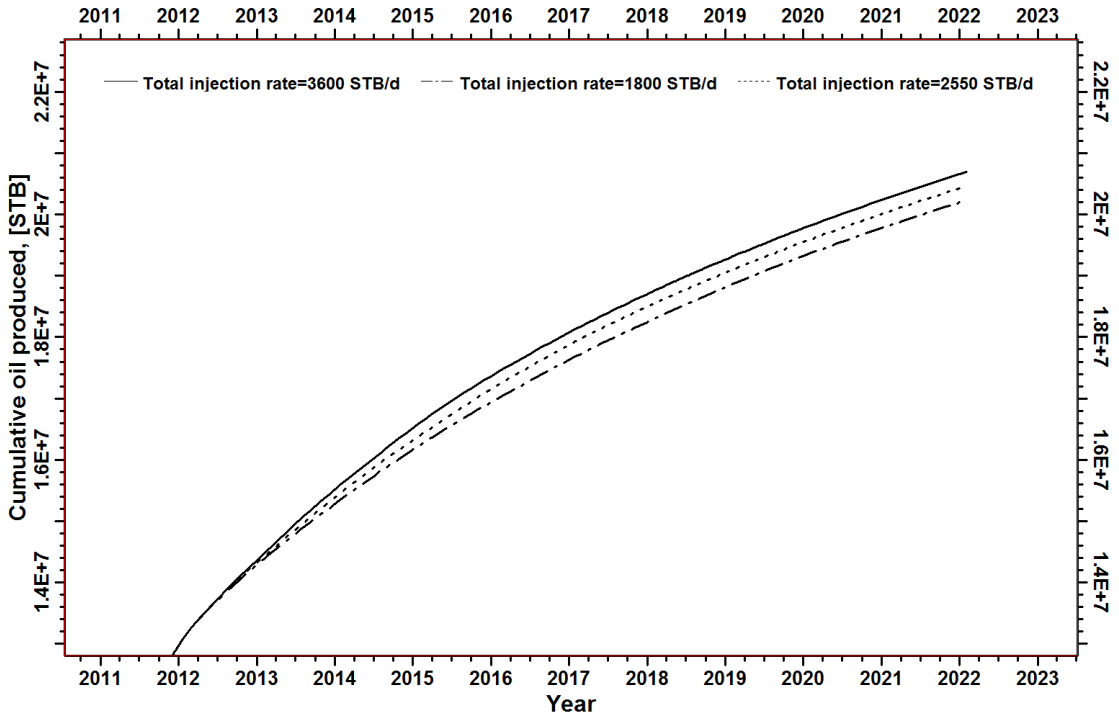

Fig. 40 — Response of the microbial boundstone reservoir cumulative oil production with changing water injection rate.

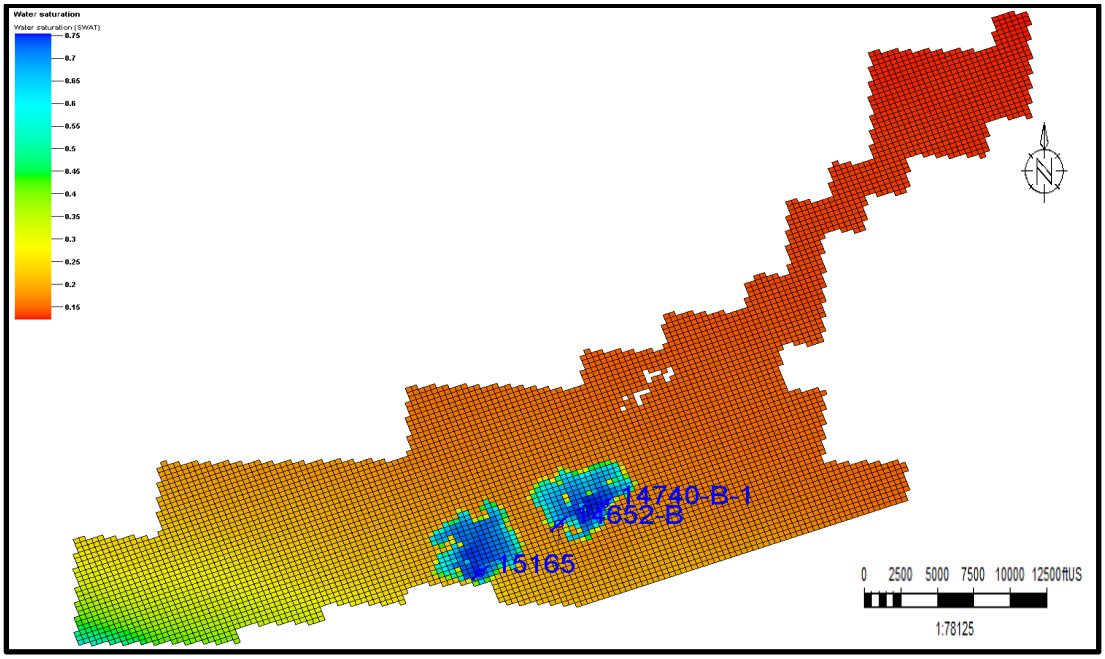

Fig. 41 — Water saturation in top of zone 11 (microbial boundstone reservoir) at the end of 5-year prediction.

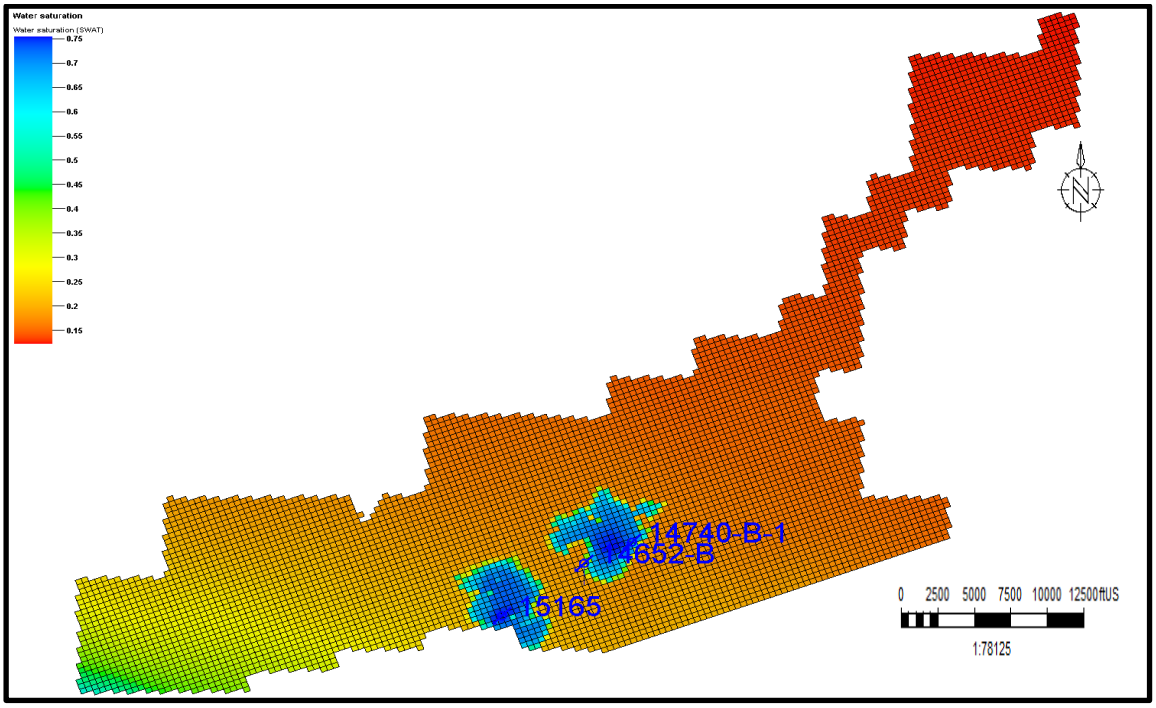

Fig. 42 — Water saturation in top of zone 12 (microbial boundstone reservoir) at the end of 5-year prediction

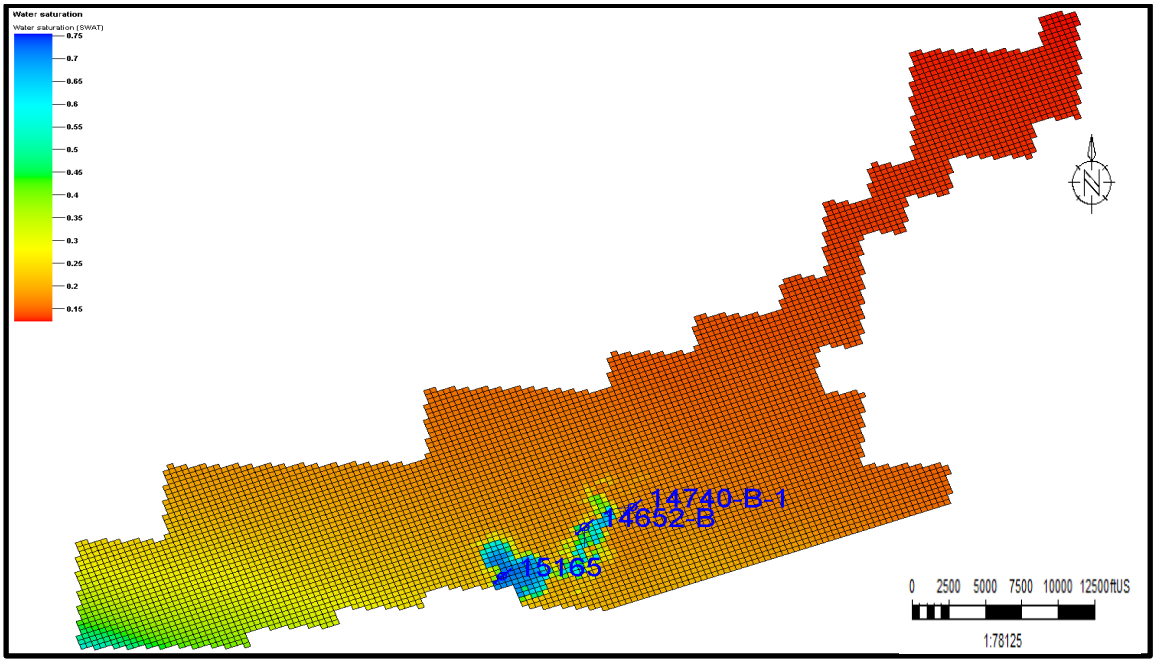

Fig. 43 — Water saturation in top of zone 13 (microbial boundstone reservoir) at the end of 5-year prediction.

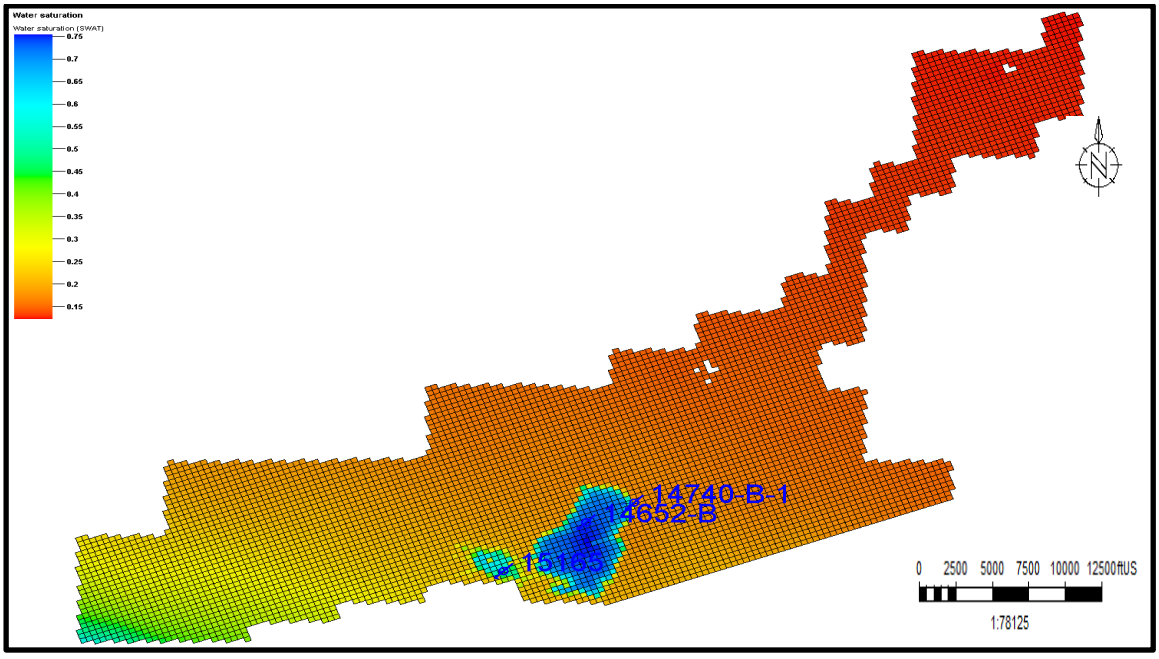

Fig. 44 — Water saturation in top of zone 14 (microbial boundstone reservoir) at the end of 5-year prediction.

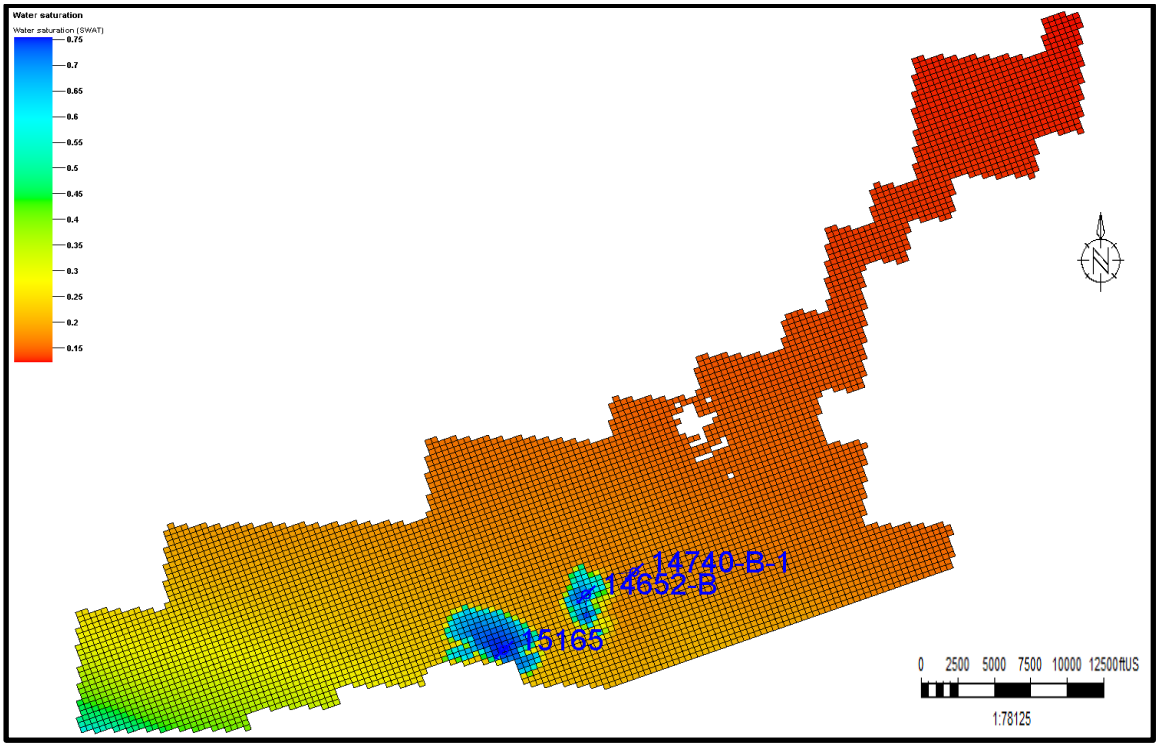

Fig. 45 — Water saturation in top of zone 15 (microbial boundstone reservoir) at the end of 5-year prediction.

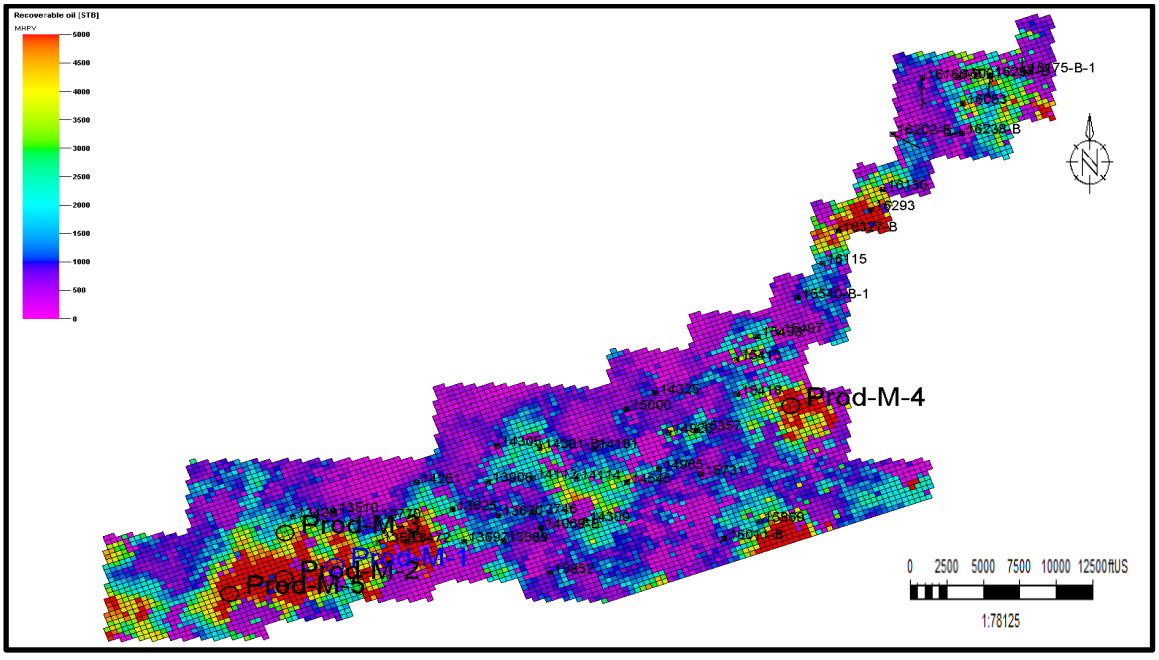

Fig. 46— MHPV in the top of zone 12 (the microbial boundstone reservoir) at the end of history matching.

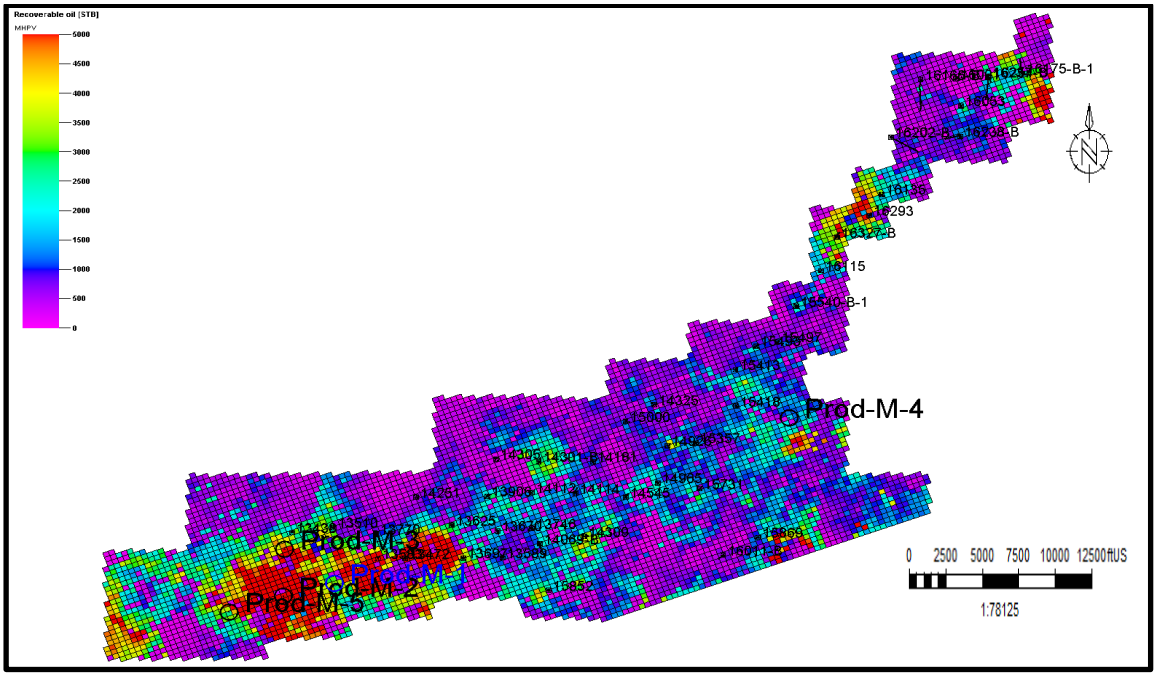

Fig. 47— MHPV in the top of zone 13 (the microbial boundstone reservoir) at the end of history matching.

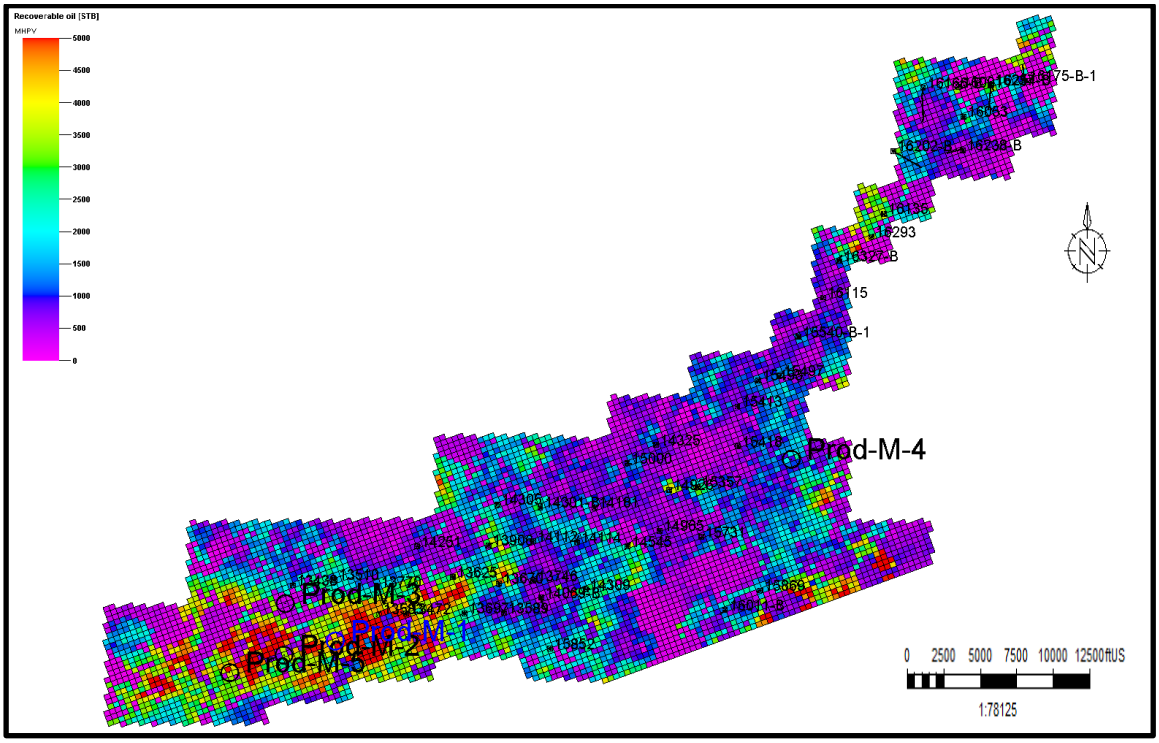

Fig. 48 — MHPV in the top of zone 14 (the microbial boundstone reservoir) at the end of history matching.

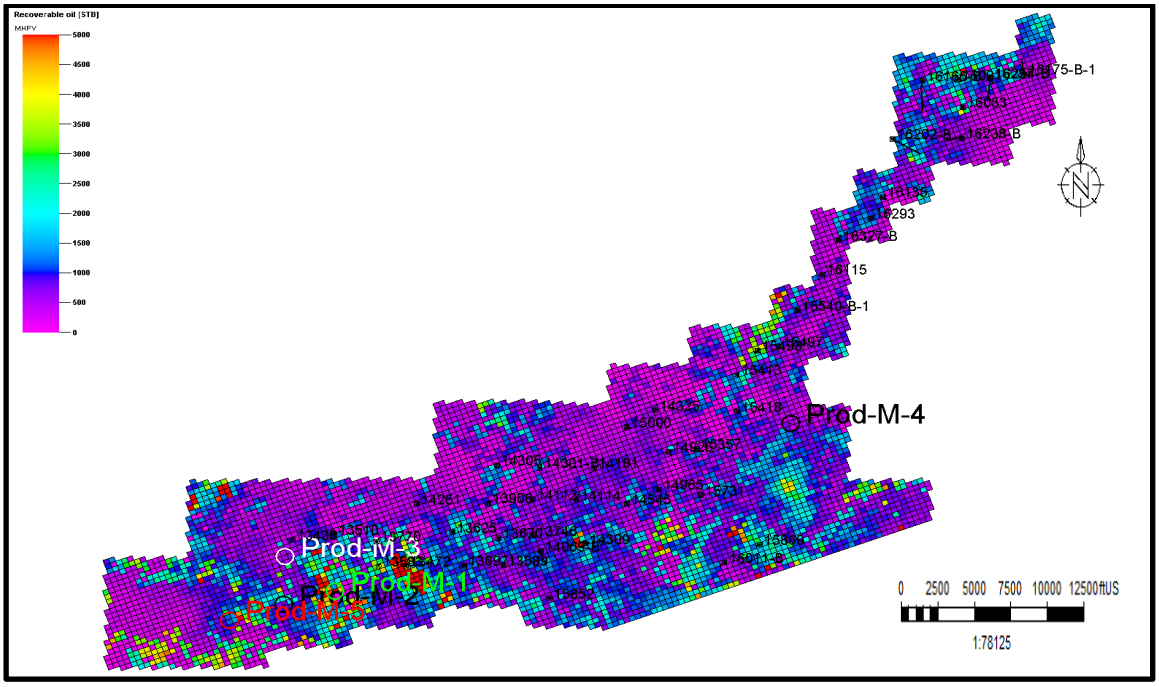

Fig. 49 — MHPV in the top of zone 15 (the microbial boundstone reservoir) at the end of history matching.

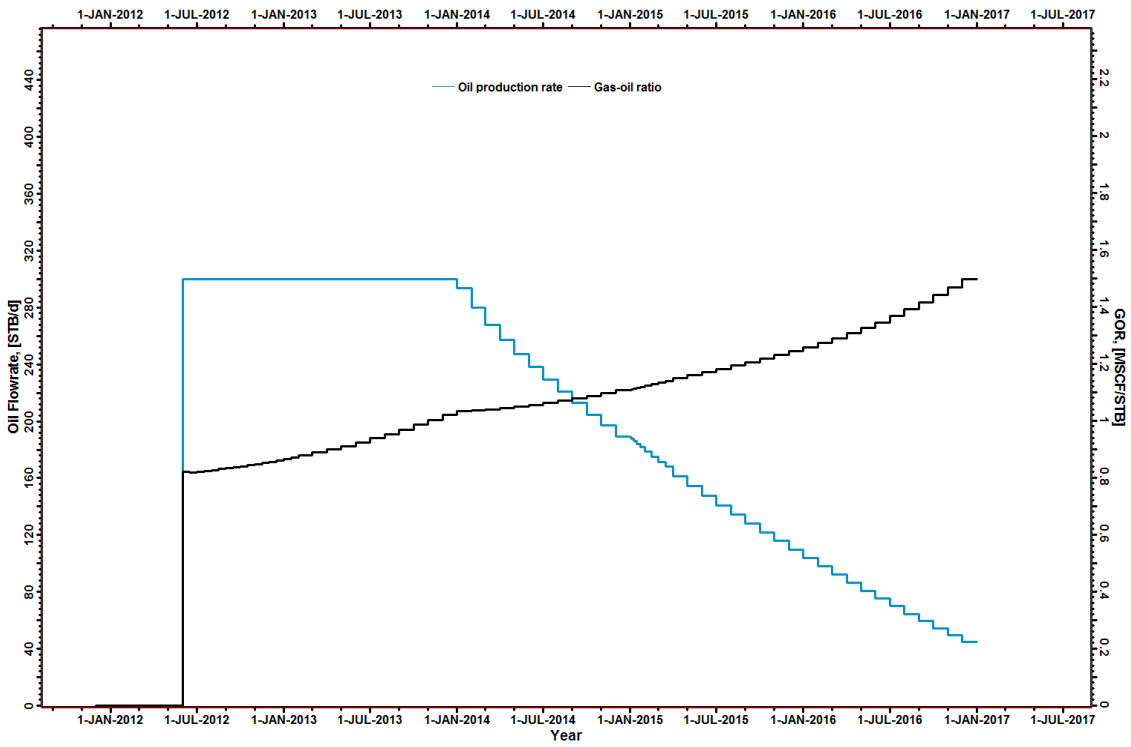

Fig. 50 — Well Prod-M-3 predicted performance.

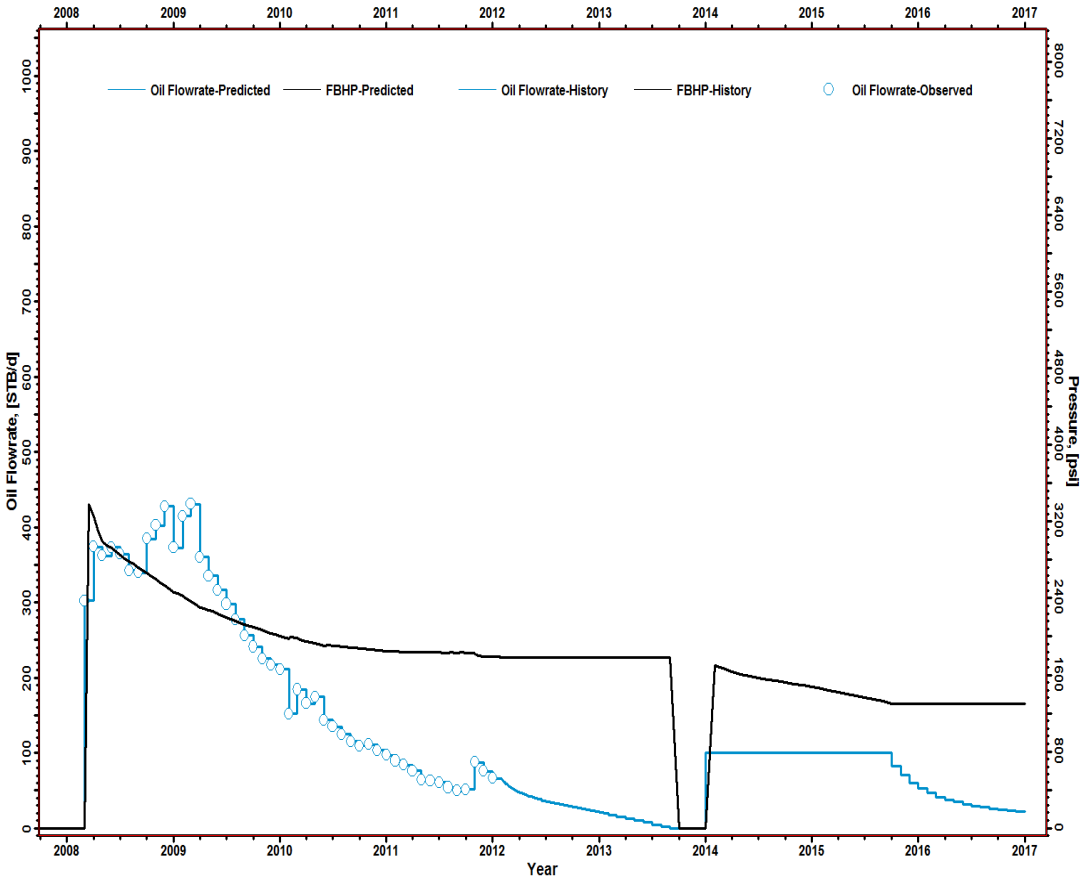

Fig. 51 — Well 15493 performance before and after work-over.

FIELD UNITIZATION

All the potential well locations investigated early in this study maintain the 160-acre unit size since the field has not been totally unitized yet. Only the southwestern portion of the field is unitized. But through this section, I discussed and showed that the field unitization and subsequent infill drilling (unit size of less than 160 acres) could result in additional oil recovery from the field.

As stated previously, the grainstone-packstone reservoir is a good candidate for infill drilling as significant oil saturation remains in inter-wells areas for wells drilled on 160 acres throughout grainstone-packstone reservoir. At least 6 potential infill wells could be drilled in the grainstone-packstone reservoir to improve recovery from the field. Appendix 1 shows the bottom hole locations of these wells. The drilling of these infill wells will result in an additional recovery up to 0.7 MMSTB of oil from the grainstone-packstone reservoir by January 2017 (**Fig. 52**).

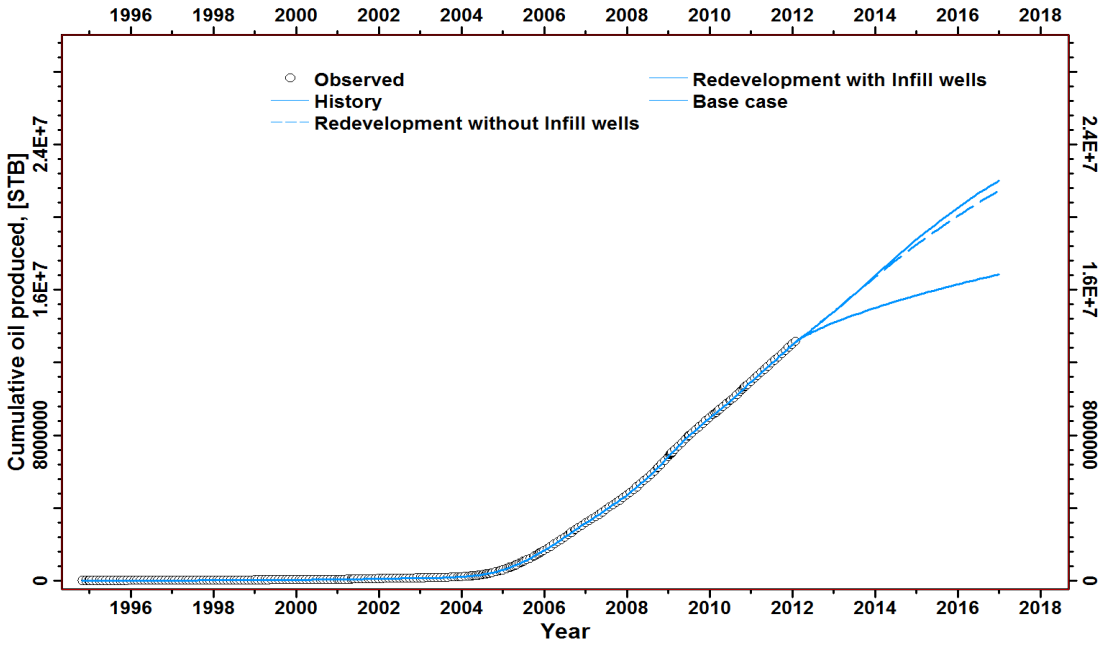

Fig. 52 — Field cumulative oil recovered vs. date

CONCLUSIONS

The reservoir simulation indicates that high remaining oil saturation exists in the lower and upper Smackover reservoirs in the Little Cedar Creek Field, especially in southwestern part of the field. Also, it indicates that a pressure maintenance program should be considered for implementation for the lower reservoir because of the continued decline in its reservoir pressure. The reservoir simulation indicates that water injection is the preferred operation pressure maintenance for the microbial boundstone (lower) reservoir rather than gas injection because of the higher permeability and connectivity present in this reservoir. The simulation studies indicate that there are numerous new well locations available for drilling on 160-acre unit size that should enhance oil recovery in the field, including 7 new well locations and 1 side track of well 10560 in the grainstone-packstone reservoir, and 5 new well locations in the microbial boundstone reservoir. Moreover, simulation studies reveal that the grainstone-packstone reservoir in the Little Cedar Creek Field is a good candidate for infill drilling. Also, production performance indicates that the microbial boundstone is more productive than the grainstone–packstone reservoir in the Little Cedar Creek Field.

Recommendations

Technically, the simulation studies show that additional oil can be recovered by the implementing the operational changes investigated in this study; however, the operator(s) of the Little Cedar Creek Field should consider the economic assessment of these operational changes to determine their economic feasibility before the implementation.

REFERENCES

Al Haddad, S. S., 2012, Reservoir Characterization, Formation Evaluation, and 3D Geologic Modeling of The Upper Jurassic Smackover Microbial Carbonate Reservoir and Associated Reservoir facies at Little Cedar Creek Field, Northeastern Gulf of Mexico: M. S. thesis, Texas A&M University, 94p.

Alabama Oil and Gas Board, 2009, An Overview of the Little Cedar Creek Field Development, [http://www.gsa.state.al.us/documents/misc_ogb/lcc_overview.pdf], 06/01/2012.

Bastian, P. A.,Gulick, K. E., Forrest, J.K. 1998, A Case History of An Integrated Study of a Mature Carbonate Waterflood, Paper presented at the 1998 SPE International Petroleum Conference and Exhibtion of Mexico, 1998.p.148-149.

Benson, D. J., 1985, Diagentic controls on reservoir development and quality, Smackover Formation of southwest Alabama: Gulf Coast Association of Geological Societies Transacations, v. 35, p. 317-326.

Dehghani, K., Harris, P. M., Edwards, K. A., and Dees, W. T.1999, Modeling a Vuggy Carbonate Reservoir, McElroy field, West Texas. American Associaton of Petroleum Geologists Bulletin, v. 83, p. 19-42.

Geological Survey of Alabma website: http://www.gsa.state.al.us/index.html

Little Cedar Creek Field PVT Reports, Geological Survey of Alabama, Dec.1994, Sept.2004, Aug.2007, Nov.2008.

MacRae, G., and Watkins, J. S., 1993, Basin architecture, Salt Tectonics, and Upper Jurassic Structural Styles, Desoto Canyon Salt Basin, Northeastern Gulf of Mexico, The American Association of Petroleum Geologist, v.77 , p.1809-1823.

Mancini, E.A., Blasingame, T.A., Rosaliand Archer, Brian J.Panetta, Juan Carlos Llinas, Charles D.Haynes, and D.Joe Benson, 2004, Improving recovery from mature oil fileds prodcuing from carboante reservoirs: Upper Jurassic Smackover Formation, Womock

Hill field, eastern Gulf Coast, USA: American Associaton of Petroleum Geologists Bulletin, v. 88, p. 1629-1651.

Mancini, E.A., W.C. Parcell, W.M. Ahr, V.O. Ramirez, J.C. Llinas and M. Cameron, 2008, Upper Jurassic updip stratigraphic trap and associated Smackover microbial and nearshore carbonate facies, eastern Gulf coastal plain: American Associaton of Petroleum Geologists Bulletin, v. 88, p. 409-434.

Mancini, E.A., and D.J. Benson, 1980, Regional stratigraphy of Upper Jurassic Smackover carbonates of southwest Alabama: Gulf Coast Association of Geological Societies Transactions, v. 30, p. 151-163.

Markland, L.A., 1992, Depositional History of the Smackover Formation, Appleton field, Escambia County, Alabama: M.S. thesis, University of Alabama, Tuscaloosa, Alabama, 145 p.

Mattax C. C., Dalton R. L.: Reservoir Simulation, SPE Monograph, Society of Petroleum Engineers, Richardson, 1990 V.13, p.44-54.

McCain,W. D., Jr 1990. The Properties of Petroleum Fluids, second Edition. PennWell Books, Tulsa,. ch.10.

McKee, D. A., 1990, Structural controls on lithofacies and petroleum geology of the Smackover Formation: Eastern Mississippi Interior Salt basin, Alabama: M. S., thesis University of Alabama, Tuscaloosa, Alabama, 254p.

Ridgway, J. G., 2010, Upper Jurassic (Oxfordian) Smackover Facies characterization at Little Cedar Creek Field, Conecuh County, Alabama: The University of Alabama MSc. Thesis, 128p.

Pindell, J., 2010, History of tectonic modelling and implications for depositional architecture in the Gulf of MmacReaexico: Where we should go from here. GCAGS Transactions,v. 60, San Antonio, Texas, p.917-929.

Wood, M. L., and J. L. Walper, 1974, The evolution of the interior Mesozoic basin and the Gulf of Mexico: Gulf Coast Association of Geological Societies Transactions, v. 24, p. 31-41.

APPENDIX 1

Well Permit	Type	Perforations	Reservoir
13583	Gas Injector	Plug back the well from bottom to depth 11,552 ft-MD Active Perforations will be 11,504-11,522 ft-MD	Upper
14740-B-1	Water Injector	11338-11350 ft-MD	Lower
14652-B	Water Injector	11588-11610 ft-MD	Lower
15165	Water Injector	Already existing perforation intervals (11552-11540, 11514-11502, 11484-11478) ft-MD. Squeeze the following intervals (11502-11514, 11478-11484) ft-MD Perforate interval (11570-11575) ft-MD	Lower

New Drilling Well Locations

Well Name/Permit	Type	Bottom Hole Location		Perforations , ft-TVDSS	Reservoir
		X,ft	Y,ft		
Prod-G-1	Oil Producer	696818.74	470003	11510.18-11540.18	Upper
Prod-G-2	Oil Producer	719747.37	484348.3	10888.94-10905.94	Upper
Prod-G-3	Oil Producer	729472.06	479686.7	10909.00-10922.00	Upper
Prod-G-4	Oil Producer	726287.6	486925.46	10764.00-10784.00	Upper
Prod-G-5	Oil Producer	719707.59	481749.07	10995.00-11010.00	Upper
Prod-G-6	Oil Producer	702412.59	476948.62	11225.00-11240.00	Upper
Prod-G-7	Oil Producer	731815.46	480604.9	10867.00-10887.00	Upper
10560	Side track	691614.93	470531.52	11542.20-11562.20	Upper
Prod-M-1	Oil Producer	700665.75	472806.25	11420.00-11440.00	Lower
Prod-M-2	Oil Producer	697405.29	471909	11495.00-11522.00	Lower
Prod-M-3	Oil Producer	697488.24	475192.85	11369.00-11385.00	Lower
Prod-M-4	Oil Producer	729661.55	484362.25	10861.00-10880.00	Lower
Prod-M-5	Oil Producer	693954.25	470800.06	11553.90-11570.90	Lower

Reference coordinates: "MENTOR: AL-W: NAD27 Alabama State Planes, Western Zone, US Foot"

Work-over Wells List

Well Permit	Reservoir
13510	Lower
13697	Lower
13770	Lower
15000	Lower
15497	Lower
16115	Lower
16135	Lower
15413	Lower
14309	Lower
14545	Lower
14965	Lower
16293	Lower
15418	Lower
15493	Lower
16327-B	Lower
16175-B-1	Lower
15540-B-1	Lower
16011-B	Lower
13625	Both
14301-B	Both
14114	Both
15068-B-1	Upper

14484	Upper
15166-B-1	Upper

Infill Well Locations

Well	Bottom hole locations	
	X, ft	Y, ft
Infill-1	722244.6	480984.97
Infill-2	725990.66	479262.8
Infill-3	711398.36	478195.36
Infill-4	714779.78	477610.51
Infill-5	718379.22	484839.58
Infill-6	728061.1	479254.83